Mathematics

http://www.aimspress.com/journal/Math

AIMS Mathematics, 11(7): 21036–21068.
DOI: 10.3934/math.2026854
Received: 07 May 2026
Accepted: 04 July 2026
Published: 16 July 2026

Research article

The impact of Lévy jumps on the dynamics of an HBV model with immune interaction and intracellular transmission pathways

Faria Mirza[1,2], **Ziyad A. Alhussain**[3,*], **Jun Feng**[1,2,*], **Anwarud Din**[4]

[1] School of Mathematical Sciences, Chengdu University of Technology, Chengdu, 610059, PR China
[2] Geomathematics Key Laboratory of Sichuan Province, Chengdu University of Technology, Chengdu, 610059, PR China
[3] Department of Statistics and Operations Research, College of Science, Qassim University, Buraydah, 52373, Saudi Arabia
[4] School of Mechanical and Electrical Engineering, Chengdu University of Technology, Chengdu, 610059, PR China

* **Correspondence:** Email: z.alhussain@qu.edu.sa, fengjun@cdut.edu.cn.

Abstract: This work develops a stochastic model to explore the dynamical behaviour of hepatitis B virus (HBV) infection by incorporating virus-to-cell transmission, cell-to-cell transmission, and the cytotoxic T lymphocyte (CTL) immune response under Lévy noise, which represents sudden environmental perturbations. The model is formulated, and its feasibility is investigated. The study is further enriched by proving the uniqueness, existence, and positivity of the global solution. A sufficient extinction condition is derived by using a combined infected-virus Lyapunov functional. In addition, a conditional sufficient criterion for long-term average persistence is established under bounded-state dynamics. The extinction result shows that infected hepatocytes and free virus particles vanish when the corresponding sufficient extinction condition is satisfied, whereas persistence is obtained under the boundedness assumption on the normalization factor and the condition $\Delta_P > 0$. At the end, numerical simulations are performed to validate and illustrate the analytical findings. Additional numerical reliability tests, including step-size sensitivity, relative error estimation, positivity verification, and comparison with a positivity-preserving truncated Euler-Maruyama scheme, are also provided. The results demonstrate that stochastic environmental perturbations can significantly affect the transmission of infectious diseases, including HBV. Significantly, excessive noise levels can greatly restrict a population's ability to spread the disease.

Keywords: cell-to-cell transmission; Lévy noise; stochastic systems; immune response; human cell; persistence; numerical analysis
Mathematics Subject Classification: 60G51, 60H10, 65C30, 68T07, 92D30

1. Introduction

Epidemics refer to the rapid spread of infectious diseases within a population over a specific period. An infectious disease is, in simple terms, a clinically verified condition caused by a pathogenic microorganism. Epidemiology, in contrast, is the systematic study of disease patterns, health-related events, and associated factors at the population level, with a particular emphasis on infectious diseases. Throughout history, epidemics have posed significant risks to human societies. For instance, in the mid-14th century, the Black Death originated in Central Asia and China before reaching England, where it claimed the lives of nearly one-third of the population within a few months [1]. Likewise, the Bombay plague (1896–1900) served as a stark reminder of the severe dangers epidemics pose to public health systems [2]. More recently, the novel coronavirus disease (COVID-19) spread to over 200 countries within a year of its emergence. As of August 29, 2020, it had resulted in approximately 25 million confirmed cases and 0.84 million deaths worldwide [3]. This ongoing global health crisis highlights the urgency and importance of strengthening efforts to prevent and control infectious diseases.

Over 350 million individuals globally are reportedly chronically infected with the hepatitis B virus (HBV) [4]. Additionally, studies show that between 25 and 40 percent of these people are chronic carriers, which puts them at risk for infections and liver-related malignancies [5]. These numbers indicate that among other medical emergencies, HBV is currently the most severe public health concern. Many researchers are trying to expand the pioneering works of Nowak et al. [5, 6] and Perelson et al. [7] for the sake to gain a better understanding of the processes of HBV transmission and therapy. Their within-host models have helped us understand how HIV and HBV are transmitted and treated. The study of several mathematical models from both dynamical and control viewpoints has helped researchers further enhance this field of study. These research studies mostly concentrate on the transmission of viruses within a single class without the usage of cells; see [8] for more information. Many models were used by Min et al. [9] and Zheng et al. [10] to find the best way to understand how HBV changes over time. They chose the conventional incidence rate over other rates, for example, the mass-action law. However, it is hard to fully understand how the disease works because a person with a chronic HBV infection usually has a serum viral load of between 2 and 3×10^{12} copies of the virus [10]. Advances in immunology and molecular medicine have revealed novel mechanisms involving extracellular vesicles and GPCR-mediated proton sensing [11, 12]. Furthermore, recent studies have identified androgen membrane receptors and developed dual antiviral-immunomodulatory therapeutics [13, 14].

We suggest considering the fact that HBV replication occurs after hepatocyte infection to explain the internal dynamics of the virus's life cycle. This delay implies that the amount of recently infected cellular populations, as opposed to the number of cells already infected at time t, dictates the inflow of virus-producing cells at that moment. Through the strength of the Cytotoxic T Lymphocyte (CTL) response, in particular, the immune system plays a critical role in regulating viral development. Even slight changes in the CTL response can greatly impact the load of infected cells and viral production. In this regard, pertinent research emphasizes that, according to Murray et al. [15], the human immune system is capable of destroying infected cells in addition to free viruses. Elaiw and AlShamrani [16] introduced a four-dimensional model that integrates the humoral immune response with a generic function. The researchers examined the global asymptotic analysis of all constant solutions using this

function. It is prominent to mention that the systems presented in [17] do not incorporate a time delay. Shi et al. [18] developed a model of HIV infection incorporating a CTL response delay and examined the effects of this time delay on equilibrium stability. Incorporating a latent period in viral models is crucial, as viruses infecting fully functional organs, like the liver, do not invariably result in immediate damage. The incubation period for HBV typically spans from six weeks to six months [19]. Several recent studies associated with vaccination and immune responses have examined molecular mechanisms, immune regulation, and potential therapeutic approaches [20–22].

Mathematical modeling serves as an essential instrument for examining the dynamics of epidemic spread and formulating effective control strategies [23, 24]. Various mathematical formulas have been explored in the past, including [25, 26], to understand HBV transmission patterns. Even though many models use deterministic methods, reference [27] shows how important it is to include environmental factors in these models to explore more thoroughly how HBV works and how to manage it. Unforeseen elements, including social dynamics and demographic traits, can intensify the transmission and effects of illnesses. As a result, the variability and uncertainty present in the environment of an epidemic can greatly affect its ongoing development and future direction. Several researchers have developed stochastic models that incorporate environmental noise [24, 25]. However, white noise cannot capture sudden and large-scale changes in the population under consideration, such as those caused by earthquakes, hazardous chemical exposure, severe weather, outbreaks of diseases such as SARS and bird flu, and similar events [25–27]. Many scientists have suggested combining Lévy noise with Gaussian white noise to overcome this constraint [28, 29]. These elements included the length of vaccine validation, the inclusion of multiple vaccination stages for long-term immunity with time intervals specified, the assessment of vaccine-related mortality, and the addition of abrupt ambient noise. The criteria required to either eliminate or keep the disease in check were also determined by this study.

Studies demonstrate that HIV and HCV disseminate within a host through two primary mechanisms: virus-to-cell infection via the extracellular milieu and cell-to-cell transmission through direct contact [30–34]. Sourisseau et al. [35] showed that cell-to-cell viral transmission in vitro happens much faster and more effectively than infection by free virus because it gets around many biophysical and kinetic barriers. Monel et al. [36] established that direct cell-to-cell transmission in vivo is more efficacious and powerful. Yang et al. [37] discussed the significance of exosomes in the transmission of HBV and the impairment of natural killer cells in individuals with chronic infection. These findings indicate that HBV infection involves both cell-to-cell and virus-to-cell transmission, as exosomes facilitate the movement of genetic material between cells. During HBV infection, uninfected hepatocytes may contract the virus by direct contact with infected hepatocytes or freshly released free viruses. The link between HBV and the cytotoxic T lymphocyte (CTL) response was described by Luzyanina and Bocharov [38] using a straightforward ordinary differential equation model. Xie et al. [39], however, examined the stochastic dynamics associated with HBV. Din [40] performed a bifurcation theory of a delayed HBV stochastic system that includes cell-to-cell transmission. This study investigates the combined effects of the CTL immune response and cell-to-cell transmission on HBV dynamics under Lévy noise.

Compared with the existing HBV stochastic models, the present study has a distinct modeling focus. The work in [25] considered a population-level HBV model with vaccination, time delay, Brownian stochastic perturbations, real data fitting, and bifurcation analysis. The work in [29] investigated the

impact of Lévy noise on a population-level HBV epidemic model and further developed a fractal-fractional Atangana-Baleanu formulation. The study in [40] is closer to the present work because it considered a within-host HBV model with virus-to-cell transmission, cell-to-cell transmission, CTL immune response, time delay, and Brownian perturbations. However, Lévy jump perturbations were not incorporated in that model. Motivated by these studies, the present work investigates a within-host HBV model involving uninfected hepatocytes, infected hepatocytes, free HBV particles, and CTL immune cells under Brownian perturbations and Lévy jump effects. The novelty of the present work does not lie in the isolated use of CTL immune response, Brownian noise, Lévy jumps, or cell-to-cell transmission, since these features have appeared separately in earlier studies. Rather, the contribution of this study is the formulation and analysis of a within-host HBV model that combines virus-to-cell transmission, cell-to-cell transmission, CTL immune response, Brownian perturbations, and a common Lévy jump source with compartment-dependent jump amplitudes. This formulation allows the model to describe continuous stochastic fluctuations together with sudden external shocks that affect the biological components of the HBV infection process with different intensities.

In order to explain the spreading behavior of HBV within the cells and to present its long-term consequences, we didies the whole population of the community into four disjoint compartments. The model divides the biological components of HBV infection into four compartments. The variable $\mathbb{X}$ represents uninfected hepatocytes, $\mathbb{Y}$ represents infected hepatocytes, $\mathbb{V}$ denotes free HBV particles, and $\mathbb{Z}$ denotes CTL immune cells. These variables are introduced here briefly and are described in detail near Eq (2.1) in Section 2. To add more complexity into the system and capture a realistic picture of the underlying biological scenario, the effect of Lévy noises were taken into account. It is widely accepted that such noises have more advantages over the standard Gaussian noises, specifically in modeling epidemic diseases where randomness in the variables behave like the assumed noise term. Introduction of jump-diffusion Lévy noise is especially noteworthy since it reveals the development of the neuron membrane. Lévy-type stochastic perturbations are shown to play a positive role in improving the stability behaviour of certian time-varying recurrent neural networks. Furthermore, such models account for the latent stage of infection, which characterizes the time-lag between an individual's exposure to the pathogenic microorganism and the eventual appearance of observable symptoms.

The main contributions of this work are summarized as follows. First, we formulate an HBV infection model that incorporates virus-to-cell transmission, cell-to-cell transmission, and CTL immune response under both Brownian perturbations and Lévy jump noise. Second, we establish the existence, uniqueness, and positivity of the global solution, which guarantees the biological feasibility of the stochastic model. Third, we derive sufficient threshold conditions for the extinction and persistence of HBV infection. Finally, we construct numerical simulations based on a Milstein-type scheme with jumps to verify the theoretical results and to illustrate the effects of stochastic perturbations on HBV dynamics. The remainder of this manuscript is structured as follows. In Section 2, we capture the dynamic of HBV through a model while incorporating Lévy noise and present the underlying assumptions of the system. Section 3 provides the required stochastic analysis and present the preliminary results needed for the subsequent discussions. The existence and uniqueness of a global positive solution of the suggested stochastic model are established in Section 4. Conditions ensuring the eradication of the disease are derived in Section 5. Section 6 is devoted to analyzing the persistence behavior of the infection within the population. To illustrate and

support the analytical results, Section 7 presents numerical simulations together with graphical illusterations. Finally, the main conclusions of the study are summarized in Section 8, where possible future research directions are also highlighted.

2. Model formulation

The HBV DNA virion infects the hepatocyte, initiating the intricate process by facilitating the transport of rcDNA. Once within the cell, the nucleus repairs the rcDNA to produce cccDNA, the necessary template for HBV replication. The transcription of cccDNA stimulates the synthesis of pgRNA, whereas reverse transcription produces ssDNA and dsDNA. This series of events highlights the complex life cycle of HBV within the host hepatocyte. The amount of the big outside antigen (P) decides where these dsDNA molecules end up. The amount determines whether dsDNA returns to the nucleus or exports as new HBV virions. Additionally, HBV can spread across hepatocytes. Infected cells, identified by their conspicuous surface antigens and double-stranded DNA, spread the virus to neighboring cells. HBV infection includes interactions with infected hepatocytes. These interactions, together with exposure to freshly released free virus, have the potential to infect non-infected hepatocytes. Din [40] created a model of HBV infection from the individual patient perspective, highlighting the CTL population, which is presented below:

$$\begin{aligned}
\frac{d\mathbb{X}}{dt} &= \Pi - \frac{\beta_1 \mathbb{X}(t)\mathbb{V}(t)}{\mathbb{N}(t)} - \frac{\beta_2 \mathbb{X}(t)\mathbb{Y}(t)}{\mathbb{N}(t)} - \mu_1 \mathbb{X}(t),\\
\frac{d\mathbb{Y}}{dt} &= \frac{\beta_1 e^{-\eta_1 \tau}\mathbb{X}(t-\tau)\mathbb{V}(t-\tau)}{\mathbb{N}(t)} + \frac{\beta_2 e^{-\eta_1 \tau}\mathbb{X}(t-\tau)\mathbb{Y}(t-\tau)}{\mathbb{N}(t)} - \alpha \mathbb{Y}(t)\mathbb{Z}(t) - \mu_2 \mathbb{Y}(t),\\
\frac{d\mathbb{V}}{dt} &= \delta \mathbb{Y}(t) - \mu_3 \mathbb{V}(t),\\
\frac{d\mathbb{Z}}{dt} &= \gamma \mathbb{Y}(t)\mathbb{Z}(t) - \mu_4 \mathbb{Z}(t).
\end{aligned} \tag{2.1}$$

The quantity $N(t)$ is used as a dimensionless normalization factor in the incidence terms, as explained below. Let $\mathbb{X}(t), \mathbb{Y}(t), \mathbb{V}(t)$, and $\mathbb{Z}(t)$ denote the concentrations at time t of uninfected hepatocytes, infected hepatocytes, free HBV particles, and CTL immune cells, respectively. More precisely, $\mathbb{X}(t)$ represents target hepatocytes that are susceptible to HBV infection, $\mathbb{Y}(t)$ represents hepatocytes infected by HBV, $\mathbb{V}(t)$ denotes the population of free virus particles released from infected cells, and $\mathbb{Z}(t)$ represents the CTL immune response responsible for eliminating infected hepatocytes. The quantity $\mathbb{N}(t)$ is used as a normalizing factor in the incidence terms. Since the model contains hepatocytes, free virus particles, and CTL immune cells, $\mathbb{N}(t)$ should not be interpreted as the total number of hepatocyte cells. The parameter Π denotes the constant recruitment rate of uninfected hepatocytes, while $(\mu_1 \mathbb{X}(t))$ represents their natural death rate. The infection of uninfected hepatocytes occurs through two routes: virus-to-cell transmission, represented by $\beta_1 \mathbb{X}(t)\mathbb{V}(t)/\mathbb{N}(t)$, and cell-to-cell transmission, represented by $\beta_2 \mathbb{X}(t)\mathbb{Y}(t)/\mathbb{N}(t)$. The parameter μ_2 denotes the natural death rate of infected hepatocytes. Infected hepatocytes are eliminated by CTL cells at the rate $\alpha \mathbb{Y}(t)\mathbb{Z}(t)$. Free virus particles are produced by infected hepatocytes at the rate $\delta \mathbb{Y}(t)$ and cleared at the rate $\mu_3 \mathbb{V}(t)$. The CTL immune response is stimulated by infected hepatocytes at the rate $\gamma \mathbb{Y}(t)\mathbb{Z}(t)$ and decays at the rate $\mu_4 \mathbb{Z}(t)$. The term τ represents a time delay accounting for the

latency in the infection process, and the factor $(e^{-\eta_1\tau})$ represents the survival probability of infected hepatocytes during the latency period.

The parameter β_2 plays an important role in the model because it describes the cell-to-cell transmission of HBV from infected hepatocytes to neighboring uninfected hepatocytes. Biologically, this route represents direct viral spread through close cellular contact, which may allow the virus to avoid some extracellular clearance mechanisms. An increase in β_2 strengthens the infection pressure on the uninfected hepatocyte population and increases the production of newly infected cells. Consequently, larger values of β_2 can increase the threshold quantities associated with persistence and make the infection more difficult to eradicate. In contrast, reducing β_2 weakens direct intracellular transmission and supports the decline of infected hepatocytes and free virus particles. Therefore, the cell-to-cell transmission rate is a key parameter governing the transition between extinction and persistence of HBV infection.

Since the present work focuses on Brownian perturbations and Lévy jump noise, we consider the non-delayed case of model (2.1). Taking $\tau = 0$ gives $e^{-\eta_1\tau} = 1$, and the delayed variables reduce to their current values. Thus, the corresponding non-delayed deterministic system is

$$\begin{aligned}
\frac{d\mathbb{X}}{dt} &= \Pi - \frac{\beta_1\mathbb{X}(t)\mathbb{V}(t)}{\mathbb{N}(t)} - \frac{\beta_2\mathbb{X}(t)\mathbb{Y}(t)}{\mathbb{N}(t)} - \mu_1\mathbb{X}(t),\\
\frac{d\mathbb{Y}}{dt} &= \frac{\beta_1\mathbb{X}(t)\mathbb{V}(t)}{\mathbb{N}(t)} + \frac{\beta_2\mathbb{X}(t)\mathbb{Y}(t)}{\mathbb{N}(t)} - \alpha\mathbb{Y}(t)\mathbb{Z}(t) - \mu_2\mathbb{Y}(t),\\
\frac{d\mathbb{V}}{dt} &= \delta\mathbb{Y}(t) - \mu_3\mathbb{V}(t),\\
\frac{d\mathbb{Z}}{dt} &= \gamma\mathbb{Y}(t)\mathbb{Z}(t) - \mu_4\mathbb{Z}(t).
\end{aligned} \tag{2.2}$$

System (2.2) is used as the deterministic baseline for the stochastic model.

The equilibrium points of system (2.2) are obtained by setting all right-hand sides equal to zero. The disease-free equilibrium is

$$\mathbb{E}_0 = \left(\frac{\Pi}{\mu_1}, 0, 0, 0\right). \tag{2.3}$$

This state represents the absence of infection: uninfected hepatocytes are present, while infected hepatocytes, free HBV particles, and CTL immune cells are absent.

The basic reproduction number of system (2.2) is obtained from the infected variables $\mathbb{Y}$ and $\mathbb{V}$ at E_0. Since $\mathbb{N}_0 = \mathbb{X}_0 = \Pi/\mu_1$, we have $\mathbb{X}_0/\mathbb{N}_0 = 1$. The linearized infected subsystem is

$$\begin{aligned}
\frac{d\mathbb{Y}}{dt} &= (\beta_2 - \mu_2)\mathbb{Y} + \beta_1\mathbb{V},\\
\frac{d\mathbb{V}}{dt} &= \delta\mathbb{Y} - \mu_3\mathbb{V}.
\end{aligned} \tag{2.4}$$

Therefore,

$$\mathbb{R}_D = \frac{\beta_2}{\mu_2} + \frac{\beta_1\delta}{\mu_2\mu_3} = \frac{\beta_1\delta + \beta_2\mu_3}{\mu_2\mu_3}. \tag{2.5}$$

Here, $\frac{\beta_2}{\mu_2}$ measures the contribution of cell-to-cell transmission, while $\frac{\beta_1\delta}{\mu_2\mu_3}$ measures the contribution of virus-to-cell transmission through free virus particles. Thus, $\mathbb{R}_D < 1$ indicates local infection extinction near $\mathbb{E}_0$, whereas $\mathbb{R}_D > 1$ indicates that the infection can invade and persist.

The positive endemic equilibrium is denoted by

$$\mathbb{E}^* = (\mathbb{X}^*, \mathbb{Y}^*, \mathbb{V}^*, \mathbb{Z}^*). \tag{2.6}$$

From the equations $\delta\mathbb{Y} - \mu_3\mathbb{V} = 0$ and $\gamma\mathbb{Y}\mathbb{Z} - \mu_4\mathbb{Z} = 0$, with $\mathbb{Z}^* > 0$, we obtain

$$\mathbb{Y}^* = \frac{\mu_4}{\gamma}, \qquad \mathbb{V}^* = \frac{\delta\mu_4}{\gamma\mu_3}. \tag{2.7}$$

Let

$$B^* = \mu_2 + \alpha\mathbb{Z}^*. \tag{2.8}$$

Then

$$\mathbb{X}^* = \frac{\Pi - \mathbb{Y}^*B^*}{\mu_1}, \qquad \mathbb{Z}^* = \frac{B^* - \mu_2}{\alpha}. \tag{2.9}$$

The value of B^* satisfies

$$\begin{aligned} &(\mu_1 - \alpha\mathbb{Y}^*)\,(B^*)^2 \\ &+ \left[\alpha\Pi + \mu_1\alpha\mathbb{Y}^*\left(1 + \frac{\delta}{\mu_3}\right) - \mu_1\mu_2 + \alpha\left(\frac{\beta_1\delta}{\mu_3} + \beta_2\right)\mathbb{Y}^*\right]B^* \\ &- \alpha\left(\frac{\beta_1\delta}{\mu_3} + \beta_2\right)\Pi = 0. \end{aligned} \tag{2.10}$$

Hence, E^* is biologically feasible when the positive root B^* satisfies

$$B^* > \mu_2, \qquad \Pi > \mathbb{Y}^*B^*. \tag{2.11}$$

In this case, all components of E^* are positive, and the equilibrium represents a chronic HBV infection state in which uninfected hepatocytes, infected hepatocytes, free virus particles, and CTL immune cells coexist.

Since the model contains different biological quantities, namely hepatocytes, free virus particles, and CTL immune cells, these variables cannot be added directly in their dimensional form. Therefore, before introducing the normalized incidence terms, we assume that the state variables have been scaled by suitable positive reference levels. More precisely, if X_c, Y_c, V_c, and Z_c denote reference concentrations for uninfected hepatocytes, infected hepatocytes, free virus particles, and CTL immune cells, respectively, then the corresponding dimensionless variables are given by

$$\widehat{X}(t) = \frac{X(t)}{X_c}, \quad \widehat{Y}(t) = \frac{Y(t)}{Y_c}, \quad \widehat{V}(t) = \frac{V(t)}{V_c}, \quad \widehat{Z}(t) = \frac{Z(t)}{Z_c}.$$

The normalization factor is then defined in terms of these dimensionless variables as

$$\widehat{N}(t) = \widehat{X}(t) + \widehat{Y}(t) + \widehat{V}(t) + \widehat{Z}(t).$$

For notational simplicity, the hats are omitted in the rest of the paper, and we write

$$\mathbb{N}(t) = \mathbb{X}(t) + \mathbb{Y}(t) + \mathbb{V}(t) + \mathbb{Z}(t).$$

Thus, $\mathbb{N}(t)$ should not be interpreted as a dimensional total population of hepatocytes, virions, and immune cells. Rather, it is a dimensionless effective normalization factor used to scale the virus-to-cell and cell-to-cell transmission terms. Under this interpretation, the transmission parameters are understood as rescaled parameters corresponding to the nondimensionalized model.

The initial conditions associated with model (2.1) are assumed to satisfy

$$(\mathbb{X}, \mathbb{Y}, \mathbb{V}, \mathbb{Z})(0) \in \mathbb{R}^4_+.$$

Under these initial conditions, the non-negativity of the solution and its boundedness on finite time intervals can be established by standard arguments.

It is widely recognized that mathematical models, irrespective of how many parameters and variables they contain, cannot fully capture the complexity of real-world problems. Consequently, discrepancies often exist between actual observations and theoretical predictions. This limitation is particularly evident in epidemic modeling, where the dynamics of the disease are frequently influenced by various environmental disturbances such as tsunamis, earthquakes, and climatic variations. These abrupt and irregular events may interrupt the continuity in the system trajectories, making classical stochastic perturbations based on Gaussian white noise insufficient to accumulate such sudden variations. For example, Shah et al. [28] showed that Lévy jump processes can improve epidemic models by capturing abrupt environmental discontinuities and sudden shocks in system behavior, which cannot be fully represented by Gaussian white noise alone. From the perspective of disease control, Lévy-type stochastic perturbations can offer valuable insights into the intrinsic randomness and sudden fluctuations that characterize the transmission of infectious diseases. Motivated by these observations, the present work incorporates Brownian perturbations and Lévy jump noise into a within-host HBV model with virus-to-cell transmission, cell-to-cell transmission, and CTL immune response, to better capture the realistic behavior of the underlying infection dynamics. However, the main aim of the present study is to investigate the independent effects of Brownian perturbations and Lévy jump noise on HBV dynamics with virus-to-cell transmission, cell-to-cell transmission, and CTL immune response. By incorporating Brownian perturbations and Lévy jump noise into system (2.2), the deterministic model is extended to the following stochastic system:

$$\begin{aligned}
d\mathbb{X}(t) &= \left[\Pi - \frac{\beta_1 \mathbb{X}(t)\mathbb{V}(t)}{\mathbb{N}(t)} - \frac{\beta_2 \mathbb{X}(t)\mathbb{Y}(t)}{\mathbb{N}(t)} - \mu_1 \mathbb{X}(t)\right]dt + \alpha_1 \mathbb{X}(t) d\mathbb{B}_1(t) + \int_Q \mathbb{S}_1(x)\mathbb{X}(t^-)\tilde{N}(d\chi_1),\\
d\mathbb{Y}(t) &= \left[\frac{\beta_1 \mathbb{X}(t)\mathbb{V}(t)}{\mathbb{N}(t)} + \frac{\beta_2 \mathbb{X}(t)\mathbb{Y}(t)}{\mathbb{N}(t)} - \alpha \mathbb{Y}(t)\mathbb{Z}(t) - \mu_2 \mathbb{Y}(t)\right]dt + \alpha_2 \mathbb{Y}(t) d\mathbb{B}_2(t)\\
&\quad + \int_Q \mathbb{S}_2(x)\mathbb{Y}(t^-)\tilde{N}(d\chi_1),\\
d\mathbb{V}(t) &= \left[\delta \mathbb{Y}(t) - \mu_3 \mathbb{V}(t)\right]dt + \alpha_3 \mathbb{V}(t) d\mathbb{B}_3(t) + \int_Q \mathbb{S}_3(x)\mathbb{V}(t^-)\tilde{N}(d\chi_1),\\
d\mathbb{Z}(t) &= \left[\gamma \mathbb{Y}(t)\mathbb{Z}(t) - \mu_4 \mathbb{Z}(t)\right]dt + \alpha_4 \mathbb{Z}(t) d\mathbb{B}_4(t) + \int_Q \mathbb{S}_4(x)\mathbb{Z}(t^-)\tilde{N}(d\chi_1),
\end{aligned} \tag{2.12}$$

where $(d\chi_1) = (dt, dx)$. Let $\mathbb{B}_i(t)$, for $i = 1, 2, 3, 4$, denote independent Brownian motion processes defined on a complete probability space $(\Omega, \mathcal{F}, \mathbb{P})$, equipped with a filtration $\{\mathcal{F}_t\}_{t\geq 0}$ satisfying the

usual conditions. The parameters α_i, for $i = 1, 2, 3, 4$, stand for the intensities of the Gaussian white noises associated with the stochastic processes. Furthermore, $\mathbb{X}(t^-)$, $\mathbb{Y}(t^-)$, $\mathbb{V}(t^-)$, and $\mathbb{Z}(t^-)$ denote the left-hand limits of the processes $\mathbb{X}(t)$, $\mathbb{Y}(t)$, $\mathbb{V}(t)$, and $\mathbb{Z}(t)$, respectively. Let $N(d\chi_1)$ be a Poisson random measure defined on a measurable subset $Q \subset [0, \infty)$ with characteristic measure ν, satisfying $\nu(Q) < \infty$. The corresponding compensated Poisson random measure is denoted by

$$\tilde{N}(d\chi_1) = N(d\chi_1) - \nu(dx)dt.$$

The functions $\mathbb{S}_i : Q \to \mathbb{R}$, for $i = 1, 2, 3, 4$, describe the magnitudes of the random jump perturbations of the system. These functions are assumed to be bounded and measurable with respect to $\mathfrak{B}(Q)$ and satisfy $\mathbb{S}_i(x) > -1$. Moreover,

$$\int_Q |\ln(1 + \mathbb{S}_i(x))|\, \nu(dx) < \infty, \qquad i = 1, 2, 3, 4.$$

These assumptions ensure that the jump terms are well defined and that the logarithmic terms appearing in Itô's formula with jumps are meaningful.
For compactness, throughout the paper we define

$$\mathcal{S}_i = \int_Q [S_i(x) - \ln(1 + S_i(x))]\nu(dx), \qquad i = 1, 2, 3, 4,$$

and

$$\mathcal{J}_i(t) = \int_0^t \int_Q \ln(1 + S_i(x))\widetilde{N}(ds, dx), \qquad i = 1, 2, 3, 4.$$

Equivalently,

$$d\mathcal{J}_i(t) = \int_Q \ln(1 + S_i(x))\widetilde{N}(dt, dx), \qquad i = 1, 2, 3, 4.$$

3. Preliminaries

This portion demonstrates some important results necessary to substantiate the study's major conclusions. Examine a full probability space $(\Omega, \mathbb{F}, \mathbb{F}_t \geq 0, P)$ with a filtration satisfying the normal criteria, namely right continuity and the inclusion of all P-null sets in $\mathbb{F}_0$. Let $y(t) \in R^n$ denote a solution to the following stochastic differential equation, now including Lévy jumps:

$$dy(t) = \mathbb{F}_1(y(t), t)dt + \mathbb{F}_2(y(t), t)d\mathbb{B}(t) + \int_{\mathbb{X}} \mathbb{F}_3(y(t^-), t, x)\tilde{N}(d\chi_1). \tag{3.1}$$

The Lévy jump term in Eq (3.1) is introduced to describe sudden and discontinuous perturbations in the system dynamics. While Brownian motion represents continuous random fluctuations, Lévy jumps account for abrupt changes caused by rare but significant environmental or biological events. In the context of HBV dynamics, such jumps may represent sudden changes in viral replication, immune response, treatment effect, or other external disturbances affecting the host environment. Therefore, including Lévy jumps allows the model to capture both continuous stochastic fluctuations and sudden shocks in the infection process.

In the above, $F_i = F_i(y(t), t)$ for $i = 1, 2$ are the measurable functions from the space $R^n \times R_+$ to R^n and $R^{n\times d}$ respectively, whereas F_3 is from the space $R^n \times R_+ \times X$ into R^n. For $t \in [0, T]$, $B(\cdot)$ represents a d-D Brownian motion, $\tilde{P}(dt, dy)$ is a one-D Poisson compensated system, and $y(t^-)$ represents the left-hand limit of the solution $y(t)$. For a given function $G \in C^{1,2}(\mathbb{R}^n \times \mathbb{R}_+; \mathbb{R}_+)$, the corresponding L-operator, obtained from SDE (3.1), may be represented as.

$$\begin{aligned} L\mathcal{G}(y,t) &= \mathcal{G}_y(y,t)F_1(y,t) + \mathcal{G}_t(y,t) + \frac{1}{2}[F_2^T(y,t)F_2(y,t)\mathcal{G}_{yy}(y,t)] \\ &\quad + \int_X [\mathcal{G}(F_3(y,t,x)+y,t) - F_3(y,t,x)\mathcal{G}_y(y,t) - \mathcal{G}(y,t)]\nu(dx), \end{aligned} \tag{3.2}$$

where $\mathcal{G}_t = \frac{\partial \mathcal{G}}{\partial t}$. $\mathcal{G}_y = (\frac{\partial \mathcal{G}}{\partial y_1}, \frac{\partial \mathcal{G}}{\partial y_2}, ..., \frac{\partial \mathcal{G}}{\partial y_n}), \mathcal{G}_{yy} = (\frac{\partial^2 \mathcal{G}}{\partial y_i \partial y_j})_{n\times n}$. Using Ito's theorem with jumps [33], the above equation becomes:

$$d\mathcal{G} = L\mathcal{G} + F_2(y,t)\mathcal{G}_y(y,t)dB(t) + \int_X [\mathcal{G}(y + F_3(y,t,z),t) - \mathcal{G}\tilde{N}(d\chi_1). \tag{3.3}$$

Lemma 3.1. *(Lemma 5.1, [41]) Let $f \in C[[0,\infty) \times \Omega, (0,\infty)]$. If there surely exists two real numbers λ_0, λ such that*

$$\log f(t) \geqslant \lambda t + \mathbb{F}(t) - \lambda_0 \int_0^t f(s)ds, \ a.s., \tag{3.4}$$

where $\mathbb{F} \in C[[0,\infty) \times \Omega, \mathbb{R}]$ and $\lim_{t\to\infty} \frac{\mathbb{F}(t)}{t} = 0$ a.s., then

$$\liminf_{t\to\infty} \frac{1}{t} \int_0^t f(s)ds \geqslant \frac{\lambda}{\lambda_0}, \ a.s. \tag{3.5}$$

4. Existence uniqueness and positivity of the solution

Establishing the presence of a non-negative solution inside the allowable zone is essential for examining the dynamic behavior of the system (2.12). Verifying that the parameters of system (2.12) adhere to the growth and Lipschitz criteria will guarantee the existence of a non-negative solution. Additional examination of Lyapunov function techniques is crucial to assess the non-locality and positivity of the solutions. By employing the approaches specified in [42], we want to conduct a thorough examination of the convergence and stability characteristics of the system, therefore improving the comprehension of its behavior. Before examining these features, we will first delineate the primary assertion and provide thorough evidence for it.

Condition 1. *For every $\mathbb{M} > 0$, there exists a constant $\mathbb{L}_\mathbb{M} > 0$ such that*

$$\int_Q \left|\mathcal{Z}_i(u,x) - \mathcal{Z}_i(\bar{u},x)\right|^2 \nu(dx) \leq \mathbb{L}_\mathbb{M}|u-\bar{u}|^2, \qquad i = 1, \ldots, 4,$$

for

$$|u| \vee |\bar{u}| \leq \mathbb{M},$$

where

$$Z_i(u,x) = S_i(x)u, \qquad u = U_i(t^-), \qquad (U_1,U_2,U_3,U_4) = (\mathbb{X},\mathbb{Y},\mathbb{V},\mathbb{Z}), \quad i = 1,\ldots,4.$$

The functions $\mathbb{S}_i : Q \to \mathbb{R}$, $i = 1,\ldots,4$, *represent the jump amplitudes associated with Lévy perturbations. Throughout this work, we assume that*

$$\mathbb{S}_i(x) > -1, \qquad i = 1,\ldots,4,$$

and

$$\int_Q |\mathbb{S}_i(x)|^2 \nu(dx) < \infty, \qquad i = 1,\ldots,4,$$

which ensure that the corresponding compensated Poisson integrals are well defined.

Condition 2. *The function*

$$|\ln(1+\mathbb{S}_i(x))|$$

is bounded, namely,

$$|\ln(1+\mathbb{S}_i(x))| \le \mathbb{C}, \qquad \mathbb{S}_i(x) > -1,$$

where $\mathbb{C}$ *is a positive constant and* $i = 1,\ldots,4$.

Theorem 4.1. *For any initial condition* $(\mathbb{X}_0,\mathbb{Y}_0,\mathbb{V}_0,\mathbb{Z}_0) \in \mathbb{R}^4_+$, *system (2.12) admits a unique global positive solution*

$$(\mathbb{X}(t),\mathbb{Y}(t),\mathbb{V}(t),\mathbb{Z}(t)) \in \mathbb{R}^4_+, \qquad t \ge 0,$$

almost surely.

Proof. By looking into the coefficients of model (2.12), we can say that it satisfies the underlying local Lipschitzness, hence Condition 1 holds for any initial values $(\mathbb{X},\mathbb{Y},\mathbb{V},\mathbb{Z})(0) \in \mathbb{R}^4_+$. For each $t \in [0,\tau_e)$, there is a unique trajectory $(\mathbb{X},\mathbb{Y},\mathbb{V},\mathbb{Z})(t)$, where τ_e is the explosion time. To demonstrate that this solution is global, $\tau_e = \infty$ must be proven. Choose a large enough integer $k_0 \ge 0$ such that the beginning values $(\mathbb{X},\mathbb{Y},\mathbb{V},\mathbb{Z})(0)$ are within the interval $\left[\frac{1}{k_0},k_0\right]$. The following stopping time is defined for each integer $k \ge k_0$:

$$\tau_k = \inf\left\{t \in [0,\tau_e) : \min\{\mathbb{X}(t),\mathbb{Y}(t),\mathbb{V}(t),\mathbb{Z}(t)\} \le \frac{1}{k} \text{ or } \max\{\mathbb{X}(t),\mathbb{Y}(t),\mathbb{V}(t),\mathbb{Z}(t)\} \ge k\right\}. \tag{4.1}$$

For the sake of simplicity, we adopt the convention that $\inf\emptyset = \infty$, where $\emptyset$ stands for the empty set. By definition, the sequence $\{\tau_k\}$ is non-decreasing as k tends to ∞. Let $\tau_\infty = \lim_{k\to\infty}\tau_k$, which implies that $\tau_\infty \le \tau_e$ almost surely. Therefore, the main objective of this theorem is to verify that $\tau_\infty = \infty$ almost surely. Suppose, on the contrary, that this claim does not hold. Then, there exist two constants $T > 0$ and $\epsilon \in (0,1)$ such that

$$P\{\tau_\infty \le T\} > \epsilon. \tag{4.2}$$

Resultantly, there exists an integer $k_1 \ge k_0$ such that

$$P\{\tau_k \le T\} > \epsilon \text{ for all } k \ge k_1. \tag{4.3}$$

Let us define a C^2-function, $\mathbb{G} : \mathbb{R}^4_+ \to \mathbb{R}_+$,

$$\mathbb{G} = (\mathbb{X} - 1 - \ln \mathbb{X}) + (\mathbb{Y} - \mathbb{C}_1 - \mathbb{C}_1 \ln \frac{\mathbb{Y}}{\mathbb{C}_1}) + \mathbb{C}_2(\mathbb{V} - 1 - \ln \frac{\mathbb{V}}{\mathbb{C}_2}) + \mathbb{C}_3(\mathbb{Z} - 1 - \ln \frac{\mathbb{Z}}{\mathbb{C}_3}). \quad (4.4)$$

Moreover, L denotes the infinitesimal generator associated with system (2.12). For each $t \in [0, \tau_k \wedge T]$, the subsequent expression is produced by applying Itô's formula onto the $\mathbb{G}$ function:

$$\begin{aligned} d\mathbb{G} &= L\mathbb{G}dt + \alpha_1(\mathbb{X} - 1)d\mathbb{B}_1(t) + \alpha_2(\mathbb{Y} - \mathbb{C}_1)d\mathbb{B}_2(t) + \alpha_3\mathbb{C}_2(\mathbb{V} - 1)d\mathbb{B}_3(t) + \alpha_4\mathbb{C}_3(\mathbb{Z} - 1)d\mathbb{B}_4(t) \\ &+ \int_Q [\mathbb{S}_1(x)\mathbb{X} - \log(1 + \mathbb{S}_1(x)) + \mathbb{S}_2(x)\mathbb{Y} - \mathbb{C}_1 \log(1 + \mathbb{S}_2(x))]\, \tilde{N}(d\chi_1) \\ &+ \int_Q [\mathbb{S}_3(x)\mathbb{V} - \mathbb{C}_2 \log(1 + \mathbb{S}_3(x)) + \mathbb{S}_4(x)\mathbb{Z} - \mathbb{C}_3 \log(1 + \mathbb{S}_4(x))]\, \tilde{N}(d\chi_1), \end{aligned} \quad (4.5)$$

where

$$\begin{aligned} L\mathbb{G} &= \left(1 - \frac{1}{\mathbb{X}}\right)\left(\Pi - \frac{\beta_1\mathbb{X}\mathbb{V}}{\mathbb{N}} - \frac{\beta_2\mathbb{X}\mathbb{Y}}{\mathbb{N}} - \mu_1\mathbb{X}\right) + \left(1 - \frac{\mathbb{C}_1}{\mathbb{Y}}\right)\left(\frac{\beta_1\mathbb{X}\mathbb{V}}{\mathbb{N}} + \frac{\beta_2\mathbb{X}\mathbb{Y}}{\mathbb{N}} - \alpha\mathbb{Y}\mathbb{Z} - \mu_2\mathbb{Y}\right) \\ &+ \left(\mathbb{C}_2 - \frac{\mathbb{C}_2}{\mathbb{V}}\right)\left(\delta\mathbb{Y} - \mu_3\mathbb{V}\right) + \left(\mathbb{C}_3 - \frac{\mathbb{C}_3}{\mathbb{Z}}\right)\left(\gamma\mathbb{Y}\mathbb{Z} - \mu_4\mathbb{Z}\right) \\ &+ \frac{\alpha_1^2 + \mathbb{C}_1\alpha_2^2 + \mathbb{C}_2\alpha_3^2 + \mathbb{C}_3\alpha_4^2}{2} + \mathcal{S}_1 + \mathbb{C}_1\mathcal{S}_2 + \mathbb{C}_2\mathcal{S}_3 + \mathbb{C}_3\mathcal{S}_4 \\ &\leq \Pi + \beta_1 + \beta_2 + \mu_1 + \mathbb{C}_1\alpha\mathbb{Z} + \mathbb{C}_1\mu_2 + \mathbb{C}_2\delta\mathbb{Y} + \mathbb{C}_2\mu_3 \\ &+ \mathbb{C}_3\gamma\mathbb{Y}\mathbb{Z} + \mathbb{C}_3\mu_4 - \alpha\mathbb{Y}\mathbb{Z} - \mu_2\mathbb{Y} - \mathbb{C}_3\mu_4\mathbb{Z} \\ &+ \frac{\alpha_1^2 + \mathbb{C}_1\alpha_2^2 + \mathbb{C}_2\alpha_3^2 + \mathbb{C}_3\alpha_4^2}{2} + \mathcal{S}_1 + \mathbb{C}_1\mathcal{S}_2 + \mathbb{C}_2\mathcal{S}_3 + \mathbb{C}_3\mathcal{S}_4. \end{aligned}$$

Let $\mathbb{C}_2\delta\mathbb{Y} - \mu_2\mathbb{Y} = 0 \Rightarrow \mathbb{C}_2 = \frac{\mu_2}{\delta}$, $\mathbb{C}_3\gamma\mathbb{Y}\mathbb{Z} - \alpha\mathbb{Y}\mathbb{Z} = 0 \Rightarrow \mathbb{C}_3 = \frac{\alpha}{\gamma}$ and $\mathbb{C}_1\alpha\mathbb{Z} - \mathbb{C}_3\mu_4\mathbb{Z} = 0 \Rightarrow \mathbb{C}_1 = \frac{\mathbb{C}_3\mu_4}{\alpha}$. Thus,

$$\begin{aligned} L\mathbb{G} &\leq \Pi + \beta_1 + \beta_2 + \mu_1 + \mathbb{C}_1\mu_2 + \mathbb{C}_2\mu_3 + \mathbb{C}_3\mu_4 \\ &+ \frac{\alpha_1^2 + \mathbb{C}_1\alpha_2^2 + \mathbb{C}_2\alpha_3^2 + \mathbb{C}_3\alpha_4^2}{2} + \mathcal{S}_1 + \mathbb{C}_1\mathcal{S}_2 + \mathbb{C}_2\mathcal{S}_3 + \mathbb{C}_3\mathcal{S}_4 = K. \end{aligned} \quad (4.6)$$

Initially, by integrating both sides of Eq (4.5) from 0 to $\tau_k \wedge T$, and subsequently computing the expectations, we obtain:

$$\mathbb{E}\left[\mathbb{G}(\mathbb{X}(\tau_k \wedge T), \mathbb{Y}(\tau_k \wedge T), \mathbb{V}(\tau_k \wedge T), \mathbb{Z}(\tau_k \wedge T))\right] \leq \mathbb{G}(\mathbb{X}_0, \mathbb{Y}_0, \mathbb{V}_0, \mathbb{Z}_0) + KT. \quad (4.7)$$

Define $\Omega_k = \{\tau_k \leq T\}$. Then, $P(\Omega_k) \geq \epsilon$ for all $k \geq k_1$. Consequently, for every ω in Ω_k, at least one component of $(\mathbb{X}(\tau_k), \mathbb{Y}(\tau_k), \mathbb{V}(\tau_k), \mathbb{Z}(\tau_k))$ is equal to $\frac{1}{k}$ or k. Thus,

$$\mathbb{G}(\mathbb{X}(\tau_k), \mathbb{Y}(\tau_k), \mathbb{V}(\tau_k), \mathbb{Z}(\tau_k)) \geq (k - 1 - \ln k) \wedge \left(\frac{1}{k} - 1 + \ln k\right).$$

According to Eq (4.7), we obtain

$$\begin{aligned}\mathbb{G}(\mathbb{X}_0, \mathbb{Y}_0, \mathbb{V}_0, \mathbb{Z}_0) + KT &\geq E[1_{\Omega_k}\mathbb{G}(\mathbb{X}(\tau_k), \mathbb{Y}(\tau_k), \mathbb{V}(\tau_k), \mathbb{Z}(\tau_k))] \\ &\geq \epsilon\left[(k - 1 - \ln k) \wedge \left(\frac{1}{k} - 1 + \ln k\right)\right].\end{aligned} \tag{4.8}$$

Letting $k \to \infty$, the right-hand side tends to infinity, while the left-hand side remains finite. This contradiction implies that $\tau_\infty = \infty$ almost surely. Hence, $\tau_e = \infty$ almost surely. Moreover, since $\mathbb{S}_i(x) > -1$, every jump changes the corresponding state variable by the multiplicative factor $1 + \mathbb{S}_i(x) > 0$. Hence, starting from positive initial data, the solution remains in $\mathbb{R}^4_+$ almost surely for all $t \geq 0$. This concludes the proof. □

Remark 4.1. *Theorem 4.1 establishes the mathematical and biological feasibility of the proposed stochastic HBV model. Since the variables $\mathbb{X}(t)$, $\mathbb{Y}(t)$, $\mathbb{V}(t)$, and $\mathbb{Z}(t)$ represent uninfected hepatocytes, infected hepatocytes, free HBV particles, and CTL immune cells, respectively, their values must remain non-negative for all time. This theorem guarantees that the solution of system (2.12) exists globally and remains in the positive region almost surely. Therefore, the subsequent extinction and persistence analyses in Sections 5 and 6 are performed on biologically meaningful solution trajectories.*

5. Extinction of the HBV infection

This section focuses on the extinction of HBV, as stated by the system (2.12), as well as establishing a threshold for forecasting illness persistence or eradication. To assist the presentation of the main conclusion, we shall introduce two critical auxiliary lemmas that are required for the proof,

$$\left\langle \mathbb{S}(t) \right\rangle = \frac{1}{t}\int_0^t \mathbb{S}(x)dx.$$

The number $\mathbb{R}_\mathbf{0}$ for the stochastic system (2.12) is calculated as

$$\mathbb{R}_\mathbf{0} = \frac{\beta_1\delta + \beta_2\mu_3}{\mu_3\left(\mu_2 + \frac{\alpha_2^2}{2} + \int_Q [S_2(x) - \ln(1 + S_2(x))]\nu(dx)\right)}. \tag{5.1}$$

When the stochastic perturbations are removed, namely $\alpha_2 = 0$ and $S_2(x) = 0$, the stochastic threshold R_0 reduces to

$$R_D = \frac{\beta_1\delta + \beta_2\mu_3}{\mu_2\mu_3},$$

which is exactly the deterministic reproduction number given in Eq (2.5).

The deterministic threshold R_D in Eq (2.5) is obtained from the deterministic system (2.2) and describes the infection invasion condition in the absence of stochastic perturbations. The quantity R_0 in Eq (5.1) is the corresponding stochastic extinction threshold for system (2.12). Compared with R_D, the denominator of R_0 contains the additional Brownian correction term $\alpha_2^2/2$ and the Lévy jump correction term

$$\int_Q [S_2(x) - \ln(1 + S_2(x))]\nu(dx).$$

Thus, stochastic perturbations increase the effective removal rate of infected hepatocytes. When these stochastic perturbations are removed, R_0 reduces exactly to R_D.

Lemma 5.1. *Let* $(\mathbb{X},\mathbb{Y},\mathbb{V},\mathbb{Z})(t)$ *denote a solution to system (2.12) with the starting condition* $(\mathbb{X},\mathbb{Y},\mathbb{V},\mathbb{Z})(0)\in\mathbb{R}^4_+$. *Subsequently, almost surely, we have*

$$\lim_{t\to\infty}\frac{\mathbb{Y}(t)+\mathbb{X}(t)+\mathbb{V}(t)+\mathbb{Z}(t)}{t}=0. \tag{5.2}$$

Moreover, if maximum$(\mu_1,\mu_2,\mu_3,\mu_4)>\frac{(\alpha_1^2\vee\alpha_2^2\vee\alpha_3^2\vee\alpha_4^2)}{2}$, *then, where* $U_1=\mathbb{X}$, $U_2=\mathbb{Y}$, $U_3=\mathbb{V}$, *and* $U_4=\mathbb{Z}$,

$$\lim_{t\to\infty}\frac{1}{t}\int_0^t U_i(u)\,d\mathbb{B}_i(u)=0,\qquad i=1,2,3,4. \tag{5.3}$$

Then,

$$\lim_{t\to\infty}\frac{\int_0^t\int_Q \mathbb{S}_i(x)U_i(s)\tilde{N}(ds,dx)}{t}=0,\qquad i=1,2,3,4. \tag{5.4}$$

Upon examination, it is noteworthy that the proof of this Lemma closely resembles the statements of Lemmas (3.1) and (5.1) in [43]. Consequently, the proofs of the lemma remain unproven in this specific instance, and one can follow [44] for a detailed proof. The following theory is crucial for the eradication of the pathogen from the population.

Theorem 5.1. *Let* $(\mathbb{X},\mathbb{Y},\mathbb{V},\mathbb{Z})(t)$ *be the positive solution of system* (2.12) *with initial data* $(\mathbb{X},\mathbb{Y},\mathbb{V},\mathbb{Z})(0)\in\mathbb{R}^4_+$. *Define*

$$\mathcal{R}_E=\frac{\beta_2\mu_3+\beta_1\delta}{\mu_2\mu_3}.$$

Assume that

$$\mathcal{R}_E<1,$$

and that the martingale convergence conditions in Lemma 5.1 hold, in particular,

$$\max(\mu_1,\mu_2,\mu_3,\mu_4)>\frac{\alpha_1^2\vee\alpha_2^2\vee\alpha_3^2\vee\alpha_4^2}{2}.$$

Then the infected hepatocyte population $\mathbb{Y}(t)$ *and the free virus population* $\mathbb{V}(t)$ *become extinct exponentially almost surely. More precisely, there exist constants* $c>0$ *and* $\rho>0$ *such that*

$$\limsup_{t\to\infty}\frac{1}{t}\log\big(\mathbb{Y}(t)+c\mathbb{V}(t)\big)\le-\rho,\qquad a.s.$$

Consequently,

$$\lim_{t\to\infty}\mathbb{Y}(t)=0,\qquad \lim_{t\to\infty}\mathbb{V}(t)=0,\qquad a.s.$$

Moreover,

$$\lim_{t\to\infty}\langle\mathbb{Y}(t)\rangle=\lim_{t\to\infty}\langle\mathbb{V}(t)\rangle=\lim_{t\to\infty}\langle\mathbb{Z}(t)\rangle=0,\qquad a.s.$$

Furthermore,

$$\lim_{t\to\infty}\langle\mathbb{X}(t)\rangle=\frac{\Pi}{\mu_1},\qquad a.s.$$

Proof. Since $\mathcal{R}_E < 1$, we have

$$\mu_2 > \beta_2 + \frac{\beta_1 \delta}{\mu_3}.$$

Hence, there exists a positive constant c such that

$$\frac{\beta_1}{\mu_3} < c < \frac{\mu_2 - \beta_2}{\delta}.$$

Define

$$a = \mu_2 - \beta_2 - c\delta > 0, \qquad b = c\mu_3 - \beta_1 > 0.$$

Let

$$\mathcal{L}(t) = \mathbb{Y}(t) + c\mathbb{V}(t).$$

Using the equations for $\mathbb{Y}(t)$ and $\mathbb{V}(t)$, we obtain

$$\begin{aligned} d\mathcal{L}(t) &= d\mathbb{Y}(t) + c\, d\mathbb{V}(t) \\ &= \left[\frac{\beta_1 \mathbb{X}(t)\mathbb{V}(t)}{\mathbb{N}(t)} + \frac{\beta_2 \mathbb{X}(t)\mathbb{Y}(t)}{\mathbb{N}(t)} - \alpha \mathbb{Y}(t)\mathbb{Z}(t) - \mu_2 \mathbb{Y}(t) + c\delta \mathbb{Y}(t) - c\mu_3 \mathbb{V}(t)\right] dt \\ &\quad + \alpha_2 \mathbb{Y}(t) d\mathbb{B}_2(t) + c\alpha_3 \mathbb{V}(t) d\mathbb{B}_3(t) \\ &\quad + \int_Q \left[S_2(x)\mathbb{Y}(t^-) + cS_3(x)\mathbb{V}(t^-)\right] \widetilde{N}(dt, dx). \end{aligned} \tag{5.5}$$

Since

$$0 \le \frac{\mathbb{X}(t)}{\mathbb{N}(t)} \le 1, \qquad \alpha \mathbb{Y}(t)\mathbb{Z}(t) \ge 0,$$

we have

$$\frac{\beta_1 \mathbb{X}(t)\mathbb{V}(t)}{\mathbb{N}(t)} \le \beta_1 \mathbb{V}(t), \qquad \frac{\beta_2 \mathbb{X}(t)\mathbb{Y}(t)}{\mathbb{N}(t)} \le \beta_2 \mathbb{Y}(t).$$

Therefore,

$$\begin{aligned} d\mathcal{L}(t) \le\ & \left[(\beta_2 - \mu_2 + c\delta)\mathbb{Y}(t) + (\beta_1 - c\mu_3)\mathbb{V}(t)\right] dt \\ & + \alpha_2 \mathbb{Y}(t) d\mathbb{B}_2(t) + c\alpha_3 \mathbb{V}(t) d\mathbb{B}_3(t) \\ & + \int_Q \left[S_2(x)\mathbb{Y}(t^-) + cS_3(x)\mathbb{V}(t^-)\right] \widetilde{N}(dt, dx). \end{aligned} \tag{5.6}$$

Using the definitions of a and b, we get

$$\begin{aligned} d\mathcal{L}(t) \le\ & \left[-a\mathbb{Y}(t) - b\mathbb{V}(t)\right] dt + \alpha_2 \mathbb{Y}(t) d\mathbb{B}_2(t) + c\alpha_3 \mathbb{V}(t) d\mathbb{B}_3(t) \\ & + \int_Q \left[S_2(x)\mathbb{Y}(t^-) + cS_3(x)\mathbb{V}(t^-)\right] \widetilde{N}(dt, dx). \end{aligned} \tag{5.7}$$

Let

$$\rho = \min\left\{a, \frac{b}{c}\right\} > 0.$$

Then

$$-a\mathbb{Y}(t) - b\mathbb{V}(t) \le -\rho\Big(\mathbb{Y}(t) + c\mathbb{V}(t)\Big) = -\rho\mathcal{L}(t). \tag{5.8}$$

Thus,

$$\begin{aligned} d\mathcal{L}(t) \leq -\rho\mathcal{L}(t)dt + \alpha_2\mathbb{Y}(t)d\mathbb{B}_2(t) + c\alpha_3\mathbb{V}(t)d\mathbb{B}_3(t) \\ + \int_Q \left[S_2(x)\mathbb{Y}(t^-) + cS_3(x)\mathbb{V}(t^-)\right]\widetilde{N}(dt,dx). \end{aligned} \tag{5.9}$$

Applying Itô's formula with jumps to $\log \mathcal{L}(t)$, we obtain

$$\begin{aligned} d\log\mathcal{L}(t) \leq -\rho\,dt - \frac{1}{2}\frac{\alpha_2^2\mathbb{Y}^2(t) + c^2\alpha_3^2\mathbb{V}^2(t)}{\mathcal{L}^2(t)}dt \\ + \int_Q \left[\log\left(1 + \frac{S_2(x)\mathbb{Y}(t^-) + cS_3(x)\mathbb{V}(t^-)}{\mathcal{L}(t^-)}\right) - \frac{S_2(x)\mathbb{Y}(t^-) + cS_3(x)\mathbb{V}(t^-)}{\mathcal{L}(t^-)}\right]\nu(dx)dt \\ + \frac{\alpha_2\mathbb{Y}(t)}{\mathcal{L}(t)}d\mathbb{B}_2(t) + \frac{c\alpha_3\mathbb{V}(t)}{\mathcal{L}(t)}d\mathbb{B}_3(t) \\ + \int_Q \log\left(1 + \frac{S_2(x)\mathbb{Y}(t^-) + cS_3(x)\mathbb{V}(t^-)}{\mathcal{L}(t^-)}\right)\widetilde{N}(dt,dx). \end{aligned}$$

Since

$$\log(1+u) - u \leq 0, \qquad u > -1,$$

and the Brownian correction term is non-positive, it follows that

$$\begin{aligned} d\log\mathcal{L}(t) \leq -\rho\,dt + \frac{\alpha_2\mathbb{Y}(t)}{\mathcal{L}(t)}d\mathbb{B}_2(t) + \frac{c\alpha_3\mathbb{V}(t)}{\mathcal{L}(t)}d\mathbb{B}_3(t) \\ + \int_Q \log\left(1 + \frac{S_2(x)\mathbb{Y}(t^-) + cS_3(x)\mathbb{V}(t^-)}{\mathcal{L}(t^-)}\right)\widetilde{N}(dt,dx). \end{aligned} \tag{5.10}$$

The logarithmic jump term is well defined. Indeed, since $S_i(x) > -1$, $i = 2, 3$, we have

$$1 + \frac{S_2(x)\mathbb{Y}(t^-) + cS_3(x)\mathbb{V}(t^-)}{\mathcal{L}(t^-)} = \frac{(1+S_2(x))\mathbb{Y}(t^-) + c(1+S_3(x))\mathbb{V}(t^-)}{\mathcal{L}(t^-)} > 0. \tag{5.11}$$

Integrating from 0 to t, we obtain

$$\frac{\log\mathcal{L}(t)}{t} \leq \frac{\log\mathcal{L}(0)}{t} - \rho + \frac{M(t)}{t},$$

where

$$\begin{aligned} M(t) = \int_0^t \frac{\alpha_2\mathbb{Y}(s)}{\mathcal{L}(s)}d\mathbb{B}_2(s) + \int_0^t \frac{c\alpha_3\mathbb{V}(s)}{\mathcal{L}(s)}d\mathbb{B}_3(s) \\ + \int_0^t\int_Q \log\left(1 + \frac{S_2(x)\mathbb{Y}(s^-) + cS_3(x)\mathbb{V}(s^-)}{\mathcal{L}(s^-)}\right)\widetilde{N}(ds,dx). \end{aligned} \tag{5.12}$$

The process $M(t)$ is a local martingale. Moreover,

$$0 \leq \frac{\mathbb{Y}(t)}{\mathcal{L}(t)} \leq 1, \qquad 0 \leq \frac{c\mathbb{V}(t)}{\mathcal{L}(t)} \leq 1.$$

Together with the boundedness assumptions on the jump amplitudes, this implies that the quadratic variation of $M(t)$ grows at most linearly in t. Therefore, by the strong law of large numbers for local martingales,

$$\lim_{t\to\infty} \frac{M(t)}{t} = 0, \qquad \text{a.s.}$$

Consequently,

$$\limsup_{t\to\infty} \frac{1}{t} \log \mathcal{L}(t) \le -\rho, \qquad \text{a.s.}$$

Since

$$\mathbb{Y}(t) \le \mathcal{L}(t), \qquad \mathbb{V}(t) \le \frac{\mathcal{L}(t)}{c},$$

we obtain

$$\lim_{t\to\infty} \mathbb{Y}(t) = 0, \qquad \lim_{t\to\infty} \mathbb{V}(t) = 0, \qquad \text{a.s.}$$

Hence,

$$\lim_{t\to\infty} \langle \mathbb{Y}(t) \rangle = \lim_{t\to\infty} \langle \mathbb{V}(t) \rangle = 0, \qquad \text{a.s.}$$

Next, applying Itô's formula with jumps to $\log \mathbb{Z}(t)$, we obtain

$$d \log \mathbb{Z}(t) = \left[\gamma \mathbb{Y}(t) - \mu_4 - \frac{\alpha_4^2}{2} - \mathcal{S}_4 \right] dt + \alpha_4 d\mathbb{B}_4(t) + d\mathcal{J}_4(t).$$

After integration and division by t, using

$$\lim_{t\to\infty} \langle \mathbb{Y}(t) \rangle = 0, \qquad \lim_{t\to\infty} \frac{\mathbb{B}_4(t)}{t} = 0, \qquad \lim_{t\to\infty} \frac{\mathcal{J}_4(t)}{t} = 0,$$

we get

$$\limsup_{t\to\infty} \frac{\log \mathbb{Z}(t)}{t} \le -\mu_4 - \frac{\alpha_4^2}{2} - \mathcal{S}_4 < 0, \qquad \text{a.s.}$$

Therefore,

$$\lim_{t\to\infty} \mathbb{Z}(t) = 0, \qquad \lim_{t\to\infty} \langle \mathbb{Z}(t) \rangle = 0, \qquad \text{a.s.} \tag{5.13}$$

Finally, integrating the equation for $\mathbb{X}(t)$ over $[0, t]$, we obtain

$$\begin{aligned} \frac{\mathbb{X}(t) - \mathbb{X}(0)}{t} = \Pi - \mu_1 \langle \mathbb{X}(t) \rangle - \left\langle \frac{\beta_1 \mathbb{X}(t) \mathbb{V}(t)}{\mathbb{N}(t)} \right\rangle - \left\langle \frac{\beta_2 \mathbb{X}(t) \mathbb{Y}(t)}{\mathbb{N}(t)} \right\rangle \\ + \frac{\alpha_1}{t} \int_0^t \mathbb{X}(s) d\mathbb{B}_1(s) + \frac{1}{t} \int_0^t \int_Q S_1(x) \mathbb{X}(s^-) \widetilde{N}(ds, dx). \end{aligned} \tag{5.14}$$

Since

$$\frac{\beta_1 \mathbb{X}(t) \mathbb{V}(t)}{\mathbb{N}(t)} \le \beta_1 \mathbb{V}(t), \qquad \frac{\beta_2 \mathbb{X}(t) \mathbb{Y}(t)}{\mathbb{N}(t)} \le \beta_2 \mathbb{Y}(t),$$

and since $\langle \mathbb{Y}(t) \rangle \to 0$ and $\langle \mathbb{V}(t) \rangle \to 0$, the two incidence averages vanish. By Lemma 5.1, the martingale terms divided by t vanish almost surely. Also, by Lemma 5.1,

$$\lim_{t\to\infty} \frac{\mathbb{X}(t) - \mathbb{X}(0)}{t} = 0, \qquad \text{a.s.} \tag{5.15}$$

Therefore,

$$\lim_{t\to\infty}\langle \mathbb{X}(t)\rangle = \frac{\Pi}{\mu_1}, \qquad \text{a.s.} \tag{5.16}$$

This completes the proof. □

Remark 5.1. *Theorem 5.1 gives a sufficient condition for the extinction of HBV infection. The proof is based on the combined infected-virus quantity $\mathcal{L}(t) = \mathbb{Y}(t) + c\mathbb{V}(t)$, which avoids unsupported ratios such as $\langle \mathbb{V}(t)\rangle/\langle \mathbb{Y}(t)\rangle$. Biologically, the condition $\mathcal{R}_E < 1$ means that the combined infection pressure from cell-to-cell and virus-to-cell transmission is weaker than the removal rates associated with infected hepatocytes and free virus particles. Hence, infected hepatocytes, free virus particles, and CTL immune cells vanish asymptotically, while the time-average level of uninfected hepatocytes approaches Π/μ_1.*

6. The persistence of the model

In contrast to deterministic models, a model founded on stochastic differential equations (SDEs) does not contain stable fixed points. Subsequently, it cannot assess the stability of the endemic equilibrium (EE), the state in which the disease persists. Researchers have employed the concept of uniqueness as an alternative approach to examine sickness persistence in stochastic models, therefore accurately depicting epidemic persistence.

Definition 6.1. *Provided that the condition specified below is satisfied, the solution of system (2.12) will continue in expectation*

$$\liminf_{t\to\infty} \frac{1}{t}\int_0^t \mathbb{Y}(r)dr > 0, \quad a.s. \tag{6.1}$$

To examine the duration of the HBV outbreak, it is advisable to consider the subsequent lemmas, as shown in [29, 41] for other illnesses as well.

Lemma 6.1. *(Strong Law [45]) Let $\mathbb{M} = \{\mathbb{M}_t\}_{t\geq 0}$ be a real-valued continuous local martingale vanishing at $t = 0$. If*

$$\lim_{t\to\infty} \left\langle \mathbb{M}, \mathbb{M}\right\rangle_t = \infty, \qquad a.s.,$$

then

$$\lim_{t\to\infty} \frac{\mathbb{M}_t}{\left\langle \mathbb{M}, \mathbb{M}\right\rangle_t} = 0, \qquad a.s.$$

Moreover, if

$$\limsup_{t\to\infty} \frac{\left\langle \mathbb{M}, \mathbb{M}\right\rangle_t}{t} < \infty, \qquad a.s.,$$

then

$$\lim_{t\to\infty} \frac{\mathbb{M}_t}{t} = 0, \qquad a.s.$$

Lemma 6.2. *Suppose $h \in \mathbb{C}([0,\infty)\times\Omega,(0,\infty))$ and $\mathbb{H} \in C([0,\infty)\times\Omega,\mathbb{R}) \ni \lim_{t\to\infty}\frac{\mathbb{H}(t)}{t} = 0$ a.s. If $\forall t \geq 0$,*

$$\ln h(t) \geq -\lambda\int_0^t h(s)ds + \lambda_0 t + \mathbb{H}(t), \quad a.s.,$$

Then,

$$\lim_{t\to\infty}\left\langle h(t)\right\rangle \geq \frac{\lambda_0}{\lambda}, \quad a.s.$$

Here, λ and λ_0 are respectively positive and non-negative real numbers.

This section discusses the long-term average persistence of the stochastic HBV model. In the revised analysis, persistence is established through a conditional sufficient criterion. Since the Lyapunov estimate contains terms involving $\mathbb{X}, \mathbb{Y}, \mathbb{V}$, and $\mathbb{Z}$, we impose explicit lower and upper bounds on the normalization factor $\mathbb{N}(t)$. These assumptions allow the nonlinear terms to be controlled rigorously and avoid the unsupported inequalities used in the previous version. The resulting persistence condition is expressed in terms of the quantity $\Delta_P > 0$.

Theorem 6.1. *Let $(\mathbb{X}, \mathbb{Y}, \mathbb{V}, \mathbb{Z})(t)$ be the positive solution of system (2.12) with initial data $(\mathbb{X}_0, \mathbb{Y}_0, \mathbb{V}_0, \mathbb{Z}_0) \in \mathbb{R}^4_+$. Define*

$$\eta_1 = \mu_1 + \frac{\alpha_1^2}{2} + \mathcal{S}_1, \qquad \eta_2 = \mu_2 + \frac{\alpha_2^2}{2} + \mathcal{S}_2,$$

and assume that $\eta_1 > 0$ and $\eta_2 > 0$. Let

$$C_1 = \frac{\Pi}{\eta_1}, \qquad C_2 = \frac{\Pi}{\eta_2}.$$

Assume further that there exist two positive constants $N_{\min}$ and $N_{\max}$, with

$$0 < N_{\min} < N_{\max},$$

such that

$$N_{\min} \leq \mathbb{N}(t) \leq N_{\max}, \qquad t \geq 0, \quad a.s.$$

Suppose that

$$\Delta_P = 2\sqrt{\frac{C_1 C_2 \Pi \beta_2}{N_{\max}}} - 2\Pi - C_1\beta_1 - C_2\alpha N_{\max} > 0.$$

Then the infected hepatocyte population $\mathbb{Y}(t)$ persists in the long-term average sense. More precisely,

$$\liminf_{t\to\infty}\langle \mathbb{Y}(t)\rangle \geq \frac{N_{\min}}{C_1\beta_2}\Delta_P > 0, \qquad a.s.$$

Proof. Define

$$\mathbb{G}_1(t) = C_1\Big(-\ln \mathbb{X}(t)\Big) + C_2\Big(-\ln \mathbb{Y}(t)\Big). \tag{6.2}$$

Applying Itô's formula with jumps to $\mathbb{G}_1(t)$, we obtain

$$d\mathbb{G}_1(t) = L\mathbb{G}_1(t)dt - C_1\alpha_1 d\mathbb{B}_1(t) - C_2\alpha_2 d\mathbb{B}_2(t) - C_1 d\mathcal{J}_1(t) - C_2 d\mathcal{J}_2(t), \tag{6.3}$$

where

$$\begin{aligned} L\mathbb{G}_1(t) = &-\frac{C_1\Pi}{\mathbb{X}(t)} + \frac{C_1\beta_1\mathbb{V}(t)}{\mathbb{N}(t)} + \frac{C_1\beta_2\mathbb{Y}(t)}{\mathbb{N}(t)} + C_1\mu_1 + \frac{C_1\alpha_1^2}{2} + C_1\mathcal{S}_1 \\ &- \frac{C_2\beta_1\mathbb{X}(t)\mathbb{V}(t)}{\mathbb{Y}(t)\mathbb{N}(t)} - \frac{C_2\beta_2\mathbb{X}(t)}{\mathbb{N}(t)} + C_2\alpha\mathbb{Z}(t) + C_2\mu_2 + \frac{C_2\alpha_2^2}{2} + C_2\mathcal{S}_2. \end{aligned} \tag{6.4}$$

Using the definitions of η_1, η_2, C_1, and C_2, we have

$$C_1\eta_1 + C_2\eta_2 = 2\Pi.$$

Therefore,

$$\begin{aligned} L\mathbb{G}_1(t) = &-\frac{C_1\Pi}{\mathbb{X}(t)} - \frac{C_2\beta_2\mathbb{X}(t)}{\mathbb{N}(t)} + 2\Pi + \frac{C_1\beta_1\mathbb{V}(t)}{\mathbb{N}(t)} + \frac{C_1\beta_2\mathbb{Y}(t)}{\mathbb{N}(t)} + C_2\alpha\mathbb{Z}(t) \\ &- \frac{C_2\beta_1\mathbb{X}(t)\mathbb{V}(t)}{\mathbb{Y}(t)\mathbb{N}(t)}. \end{aligned} \tag{6.5}$$

By the arithmetic–geometric mean inequality,

$$-\frac{C_1\Pi}{\mathbb{X}(t)} - \frac{C_2\beta_2\mathbb{X}(t)}{\mathbb{N}(t)} \le -2\sqrt{\frac{C_1C_2\Pi\beta_2}{\mathbb{N}(t)}}.$$

Since $\mathbb{N}(t) \le N_{\max}$, we get

$$-2\sqrt{\frac{C_1C_2\Pi\beta_2}{\mathbb{N}(t)}} \le -2\sqrt{\frac{C_1C_2\Pi\beta_2}{N_{\max}}}.$$

Moreover, because all state variables are nonnegative and

$$\mathbb{N}(t) = \mathbb{X}(t) + \mathbb{Y}(t) + \mathbb{V}(t) + \mathbb{Z}(t),$$

we have

$$\frac{\mathbb{V}(t)}{\mathbb{N}(t)} \le 1, \qquad \mathbb{Z}(t) \le \mathbb{N}(t) \le N_{\max}, \qquad \frac{\mathbb{Y}(t)}{\mathbb{N}(t)} \le \frac{\mathbb{Y}(t)}{N_{\min}}.$$

Also,

$$-\frac{C_2\beta_1\mathbb{X}(t)\mathbb{V}(t)}{\mathbb{Y}(t)\mathbb{N}(t)} \le 0.$$

Hence,

$$\begin{aligned} L\mathbb{G}_1(t) &\le -2\sqrt{\frac{C_1C_2\Pi\beta_2}{N_{\max}}} + 2\Pi + C_1\beta_1 + C_2\alpha N_{\max} + \frac{C_1\beta_2}{N_{\min}}\mathbb{Y}(t) \\ &= -\Delta_P + \frac{C_1\beta_2}{N_{\min}}\mathbb{Y}(t). \end{aligned} \tag{6.6}$$

Thus,

$$d\mathbb{G}_1(t) \le \left[-\Delta_P + \frac{C_1\beta_2}{N_{\min}}\mathbb{Y}(t)\right]dt + dM(t),$$

where

$$M(t) = -C_1\alpha_1\mathbb{B}_1(t) - C_2\alpha_2\mathbb{B}_2(t) - C_1\mathcal{J}_1(t) - C_2\mathcal{J}_2(t) \tag{6.7}$$

is a local martingale. Integrating from 0 to t, we obtain

$$\mathbb{G}_1(t) - \mathbb{G}_1(0) \le -\Delta_P t + \frac{C_1\beta_2}{N_{\min}}\int_0^t \mathbb{Y}(s)\,ds + M(t).$$

Dividing by t, we get

$$\frac{C_1\beta_2}{N_{\min}}\langle \mathbb{Y}(t)\rangle \geq \Delta_P + \frac{\mathbb{G}_1(t)-\mathbb{G}_1(0)}{t} - \frac{M(t)}{t}.$$

Since $\mathbb{X}(t) \leq N_{\max}$ and $\mathbb{Y}(t) \leq N_{\max}$, the function $\mathbb{G}_1(t)$ is bounded from below. Hence,

$$\liminf_{t\to\infty} \frac{\mathbb{G}_1(t)-\mathbb{G}_1(0)}{t} \geq 0.$$

Moreover, by the strong law of large numbers for local martingales,

$$\lim_{t\to\infty} \frac{M(t)}{t} = 0, \qquad \text{a.s.}$$

Consequently,

$$\liminf_{t\to\infty}\langle \mathbb{Y}(t)\rangle \geq \frac{N_{\min}}{C_1\beta_2}\Delta_P > 0, \qquad \text{a.s.} \tag{6.8}$$

This proves that the infected hepatocyte population persists in the long-term average sense. □

Remark 6.1. *Theorem 6.1 provides a conditional sufficient criterion for the persistence of HBV infection in the stochastic model. In contrast to the previous version, the revised proof explicitly assumes upper and lower bounds for the normalization factor $\mathbb{N}(t)$. These assumptions are used to control the terms involving $\mathbb{X}, \mathbb{Y}, \mathbb{V}$, and $\mathbb{Z}$, thereby avoiding the unjustified inequalities in the earlier proof. Therefore, the revised persistence result should be interpreted as a sufficient persistence condition under bounded-state dynamics.*

7. Numerical analysis

The present part of the manuscript has two primary purposes. The first is to design an appropriate numerical scheme for simulating model (2.12). The second purpose is to provide representative numerical examples that explain the influence of various system components on the model dynamics. Through these simulations, we obtain a clearer scenario of the qualitative behavior of the model and the manner in which its parameters govern the evolution of the underlying epidemiological process.

7.1. Milstein scheme with jumps

To obtain approximate solutions of model (2.12), we employ the numerical scheme introduced in [43]. This technique has been successfully applied to several models in the literature, as reported in [44–46], demonstrating the reliability of the method for stochastic systems with jump components. In order to implement this scheme, we consider the following settings: let $x^* \in \mathcal{S}$ stand for a representative point in the jump space, and let $\mathbb{N}^*$ represent a positive integer. The discrete index n takes values from the set $\{0, 1, 2, \ldots, \mathbb{N}^*\}$. The time interval $[0, T]$ is divided into $\mathbb{N}^*$ equal subintervals, each having length $\Delta t = \frac{T}{\mathbb{N}^*}$, which defines the step size of the numerical process. Let $\mathbb{N}^n = \mathbb{X}^n + \mathbb{Y}^n + \mathbb{V}^n + \mathbb{Z}^n$ represent the total effective population at the discrete time level t_n. The increment of the Brownian motions, denoted by $\Delta\mathbb{B}_{i,n} = \mathbb{B}_i(t_{n+1}) - \mathbb{B}_i(t_n)$, is generated by

$$\Delta\mathbb{B}_{i,n} = \sqrt{\Delta t}\,\xi_{i,n},$$

where $\xi_{i,n}$ are independent standard Gaussian random variables with mean 0 and variance 1. In addition, the jump increment $\Delta\mathbb{L}_n = \mathbb{L}(t_{n+1}) - \mathbb{L}(t_n)$ follows a Poisson distribution with intensity parameter $\nu\Delta t$. The jump space is taken as $Q = (0, \infty)$, and the corresponding intensity measure satisfies $\nu(Q) < \infty$. With these definitions, the Milstein numerical scheme corresponding to model (2.12) can be written as follows:

$$\begin{aligned}
\mathbb{X}^{n+1} &= \mathbb{X}^n + \left[\Pi - \frac{\beta_1 \mathbb{X}^n \mathbb{V}^n}{\mathbb{N}^n} - \frac{\beta_2 \mathbb{X}^n \mathbb{Y}^n}{\mathbb{N}^n} - \mu_1 \mathbb{X}^n\right]\Delta t \\
&\quad + \alpha_1 \mathbb{X}^n \Delta\mathbb{B}_{1,n} + \frac{\alpha_1^2}{2}\mathbb{X}^n\left((\Delta\mathbb{B}_{1,n})^2 - \Delta t\right) + \mathbb{S}_1(x^*)\mathbb{X}^n\Delta\mathbb{L}_n, \\
\mathbb{Y}^{n+1} &= \mathbb{Y}^n + \left[\frac{\beta_1 \mathbb{X}^n \mathbb{V}^n}{\mathbb{N}^n} + \frac{\beta_2 \mathbb{X}^n \mathbb{Y}^n}{\mathbb{N}^n} - \alpha\mathbb{Y}^n\mathbb{Z}^n - \mu_2\mathbb{Y}^n\right]\Delta t + \alpha_2\mathbb{Y}^n\Delta\mathbb{B}_{2,n} \\
&\quad + \frac{\alpha_2^2}{2}\mathbb{Y}^n\left((\Delta\mathbb{B}_{2,n})^2 - \Delta t\right) + \mathbb{S}_2(x^*)\mathbb{Y}^n\Delta\mathbb{L}_n, \\
\mathbb{V}^{n+1} &= \mathbb{V}^n + \left[\delta\mathbb{Y}^n - \mu_3\mathbb{V}^n\right]\Delta t + \alpha_3\mathbb{V}^n\Delta\mathbb{B}_{3,n} + \frac{\alpha_3^2}{2}\mathbb{V}^n\left((\Delta\mathbb{B}_{3,n})^2 - \Delta t\right) + \mathbb{S}_3(x^*)\mathbb{V}^n\Delta\mathbb{L}_n, \\
\mathbb{Z}^{n+1} &= \mathbb{Z}^n + \left[\gamma\mathbb{Y}^n\mathbb{Z}^n - \mu_4\mathbb{Z}^n\right]\Delta t + \alpha_4\mathbb{Z}^n\Delta\mathbb{B}_{4,n} + \frac{\alpha_4^2}{2}\mathbb{Z}^n\left((\Delta\mathbb{B}_{4,n})^2 - \Delta t\right) + \mathbb{S}_4(x^*)\mathbb{Z}^n\Delta\mathbb{L}_n.
\end{aligned}$$

Here, $\mathbb{S}_i(x^*)\Delta\mathbb{L}_n$, for $i = 1, 2, 3, 4$, represents the discrete approximation of the jump perturbation associated with the jump amplitude function $\mathbb{S}_i(x)$ in model (2.12). Thus, the jump terms in the numerical scheme are directly linked to the Lévy jump functions introduced in the stochastic model. To maintain consistency with the theoretical positivity of the continuous model, the simulations were performed using a sufficiently small time step, and the non-negativity condition was enforced on the numerical trajectories whenever small negative values appeared due to discretization error.

The numerical scheme employed in this work is not the only available procedure for obtaining approximate solutions of such models. Another well-known and effective alternative method is the positivity-preserving truncated Euler-Maruyama (PPTEM) method [46]. This technique has been widely used in the existing literature and has proven to be a reliable tool for handling complex stochastic models, particularly those involving jump perturbations and nonlinear dynamics [44–46]. For the purpose of performing numerical simulations of system (2.12), we considered the following values of the parameters and initial conditions.

The parameter values and initial conditions used in Sections 7.2–7.5 are given in Table 1.

Table 1. Parameter values and initial conditions used in the numerical simulations of model (2.12). Here, (μL^{-1}) denotes concentration per microliter.

Parameters	Set 1	Set 2	Set 3	Unit	Source
Π	1.50	5.00	5.00	μ L $^{-1}$ per day	Assumed
β_1	0.01	0.70	1.00	μL^{-1} per day	[40]
β_2	0.03	0.50	1.0	μL^{-1} per day	Assumed
μ_1	0.20	0.30	0.01	day^{-1}	Assumed
μ_2	0.20	0.60	0.20	per day	[40]
μ_3	0.40	0.30	1.00	per day	Assumed
μ_4	0.60	0.02	0.80	per day	Assumed
α	0.09	0.90	0.20	μL^{-1} per day	[40]
δ	0.0005	0.10	0.20	per day	Assumed
γ	0.001	0.20	0.20	per day	Assumed
α_1	0.09	0.60	–	–	Assumed
α_2	0.05	0.60	–	–	Assumed
α_3	0.03	0.60	–	–	Assumed
α_4	0.05	0.60	–	–	Assumed
$\mathbb{X}_0$	0.50	0.500	0.50	–	Assumed
$\mathbb{Y}_0$	0.70	0.70	0.70	–	Assumed
$\mathbb{V}_0$	0.05	0.05	0.05	–	Assumed
$\mathbb{Z}_0$	0.03	0.03	00.03	–	Assumed

7.2. Step-size sensitivity, error estimate, and positivity verification

To examine the numerical reliability of the proposed Milstein-type scheme with jumps, we performed additional step-size sensitivity tests for

$$\Delta t = 0.10, \quad 0.05, \quad 0.025.$$

Since the exact solution of the stochastic jump system is not available, the numerical error was estimated by comparing solutions obtained under successive time-step refinements. The Brownian and Poisson increments were generated on the finest time grid and then aggregated for the coarser time steps, so that the solutions were compared under the same stochastic sample path. For each state variable $U_i \in \{X, Y, V, Z\}$, the relative error was computed as

$$E_i(\Delta t) = \frac{\left(\sum_{n=0}^{N} \left|U_i^{\Delta t}(t_n) - U_i^{\Delta t/2}(t_n)\right|^2\right)^{1/2}}{\left(\sum_{n=0}^{N} \left|U_i^{\Delta t/2}(t_n)\right|^2\right)^{1/2}}.$$

The total error was defined by

$$E(\Delta t) = E_X(\Delta t) + E_Y(\Delta t) + E_V(\Delta t) + E_Z(\Delta t).$$

The results are reported in Table 2. The total relative error decreases from 1.8058×10^{-2} to 1.1378×10^{-2} as the time step is refined, which supports the numerical consistency of the scheme.

Table 2. Step-size sensitivity and relative numerical error for the Milstein-type scheme with jumps.

Comparison	E_X	E_Y	E_V	E_Z	Total error
0.10 vs 0.05	1.1467×10^{-3}	1.2871×10^{-3}	7.3916×10^{-3}	8.2323×10^{-3}	1.8058×10^{-2}
0.05 vs 0.025	6.6927×10^{-4}	3.0264×10^{-3}	3.7194×10^{-3}	3.9631×10^{-3}	1.1378×10^{-2}

The positivity of the numerical trajectories was also checked by recording the minimum values of all state variables. As shown in Table 3, the variables remain nonnegative for all tested time steps. The very small values 2.2204×10^{-16} correspond to machine precision, indicating that the infected hepatocytes, free virus particles, and CTL immune cells approach the extinction level numerically. The normalization factor $N(t)$ also remains bounded during the simulations.

Table 3. Positivity and boundedness check for different time steps.

Δt	$\min X$	$\min Y$	$\min V$	$\min Z$	$\min N$	$\max N$
0.10	0.5000	2.2204×10^{-16}	2.2204×10^{-16}	2.2204×10^{-16}	1.2800	14.5640
0.05	0.5000	2.2204×10^{-16}	2.2204×10^{-16}	2.2204×10^{-16}	1.2800	14.5410
0.025	0.5000	2.2204×10^{-16}	2.2204×10^{-16}	2.2204×10^{-16}	1.2800	14.6020

Finally, the Milstein-type scheme was compared with a positivity-preserving truncated Euler-Maruyama scheme. The comparison is shown in Table 4. Both schemes preserve nonnegativity and lead to the same qualitative extinction behavior. The final values of $Y(t)$ and $V(t)$ are close to machine precision in both methods.

Table 4. Comparison between the Milstein-type scheme and the positivity-preserving truncated Euler-Maruyama scheme.

Scheme	Minimum value	Final $Y(t)$	Final $V(t)$
Milstein-type scheme with jumps	2.2204×10^{-16}	2.5814×10^{-16}	2.2204×10^{-16}
PPTEM scheme with jumps	2.2204×10^{-16}	2.5826×10^{-16}	2.2204×10^{-16}

The relative difference between the Milstein-type scheme and the PPTEM scheme is

$$E_X = 3.0 \times 10^{-3}, \quad E_Y = 6.5083 \times 10^{-4}, \quad E_V = 2.8368 \times 10^{-4}, \quad E_Z = 3.3780 \times 10^{-4},$$

with total relative difference 4.2×10^{-3}. Hence, the extinction behavior is not an artifact of the chosen discretization method.

7.3. Numerical simulation of extinction

By using the above scheme and the suggested values of the parameters, numerical simulations have been conducted to support the theoretical outcomes for models (2.12) and (2.1) and to corroborate the extinction criteria stated in Theorem 5.1. The discretization time step used in the simulations is chosen as $\Delta t = 0.10$. The initial values and parameters of model (2.12) are based on those reported in Table 1 (Set 1), while $h_1 = 0.02$, $h_2 = 0.06$, $h_3 = 0.004$, and $h_4 = 0.04$. Under these parameter settings, the basic threshold parameter R_0 satisfies $R_0 < 1$. According to Theorem 5.1, this condition guarantees that the infection will eventually dies out from the population. In other words, the solution trajectories converge to zero as time evolves, indicating the gradual eradication of the infection. The numerical results explaining this behavior are outlines in Fig. 1. Over time, HBV treatment may not benefit everyone, including the same patient. To account for this variation, we may incorporate Lévy noise in the model. Lévy noise, which displays random fluctuations or unpredictability in a stochastic environment, can come from a number of sources. Interestingly, increasing the amount of white noise can have a noticeable impact on the system's dynamics, such as speeding up the killing of HBV-infected cells. External factors that create volatility or unpredictability in the environment can results an increase in Lévy noise within the model.

The nearly flat profiles of $\mathbb{Y}(t)$, $\mathbb{V}(t)$, and $\mathbb{Z}(t)$ in Figure 1 are a consequence of the extinction condition $R_0 < 1$. Under the parameter values of Table 1 (Set 1), the infected hepatocyte population, free virus particles, and CTL immune response decay rapidly during the early stage of the simulation. Therefore, over the longer interval $0 \leq t \leq 600$, these trajectories remain close to zero and appear nearly empty in the corresponding panels. This behavior is consistent with Theorem 5.1, which predicts extinction of the infection when $R_0 < 1$. In contrast, the persistence cases shown in the subsequent figures exhibit nonzero trajectories over time.

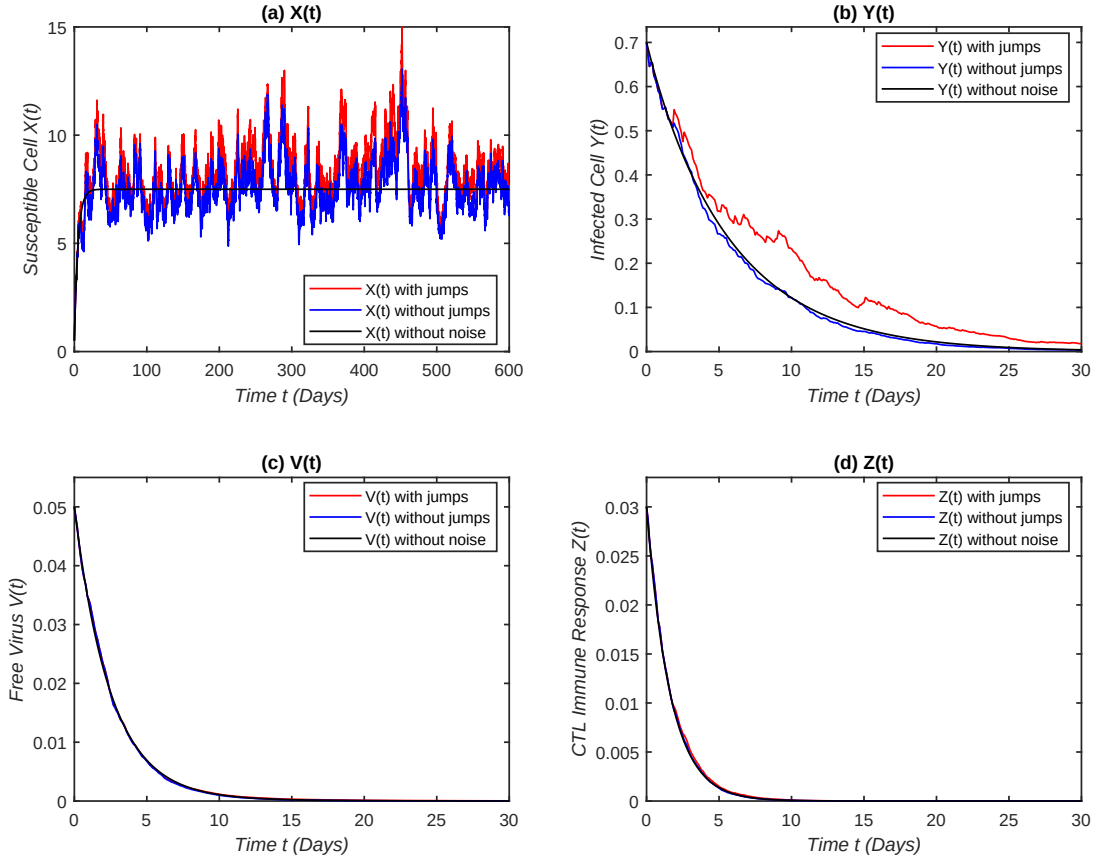

Figure 1. Extinction dynamics of the state variables of system (2.12) under the parameter values of Table 1 (Set 1), where $R_0 < 1$. Panel (a) shows the trajectory of uninfected hepatocytes $\mathbb{X}(t)$ over the full time interval $0 \le t \le 600$. Panels (b)–(d) show zoomed early-time trajectories of infected hepatocytes $\mathbb{Y}(t)$, free virus particles $\mathbb{V}(t)$, and CTL immune cells $\mathbb{Z}(t)$, respectively, over $0 \le t \le 30$, in order to make the transient behavior and the differences among the cases with Lévy jumps, without jumps, and without stochastic noise visible. The results show that $\mathbb{Y}(t)$, $\mathbb{V}(t)$, and $\mathbb{Z}(t)$ approach zero, confirming the extinction behavior predicted by Theorem 5.1.

7.4. Numerical simulation of persistence

To illustrate the persistence behaviour numerically, simulations are performed using the initial conditions and parameter values listed in Table 1 (Set 2) for system (2.12). In this case, the parameters h_i's are chosen as $h_1 = 0.02$, $h_2 = 0.03$, $h_3 = 0.004$, and $h_4 = 0.05$. The numerical trajectories show that the infected hepatocytes and free virus particles remain positive over long time intervals. This behaviour is consistent with the conditional persistence result in Theorem 6.1 under bounded-state dynamics. The corresponding trajectories are shown in Figure 2.

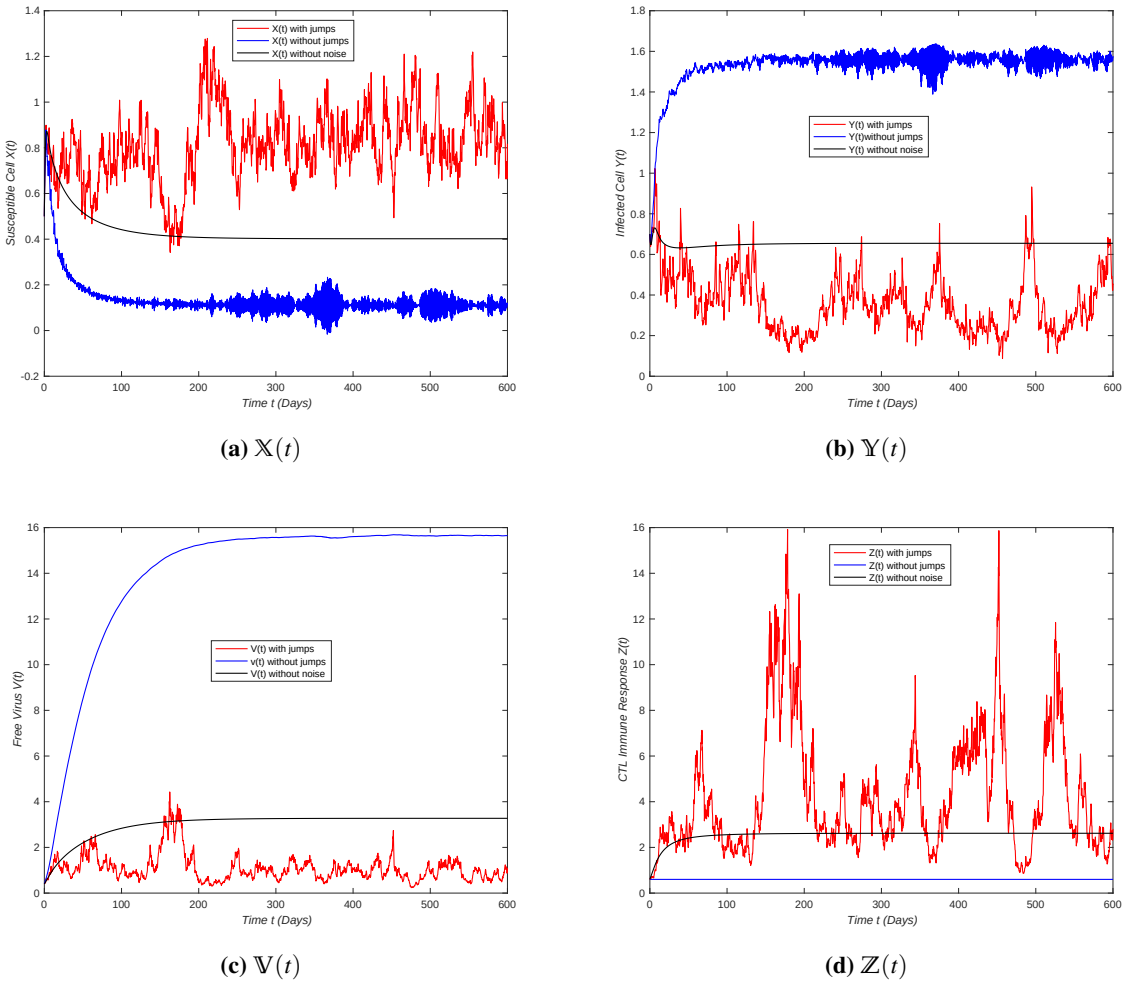

(a) $\mathbb{X}(t)$ **(b)** $\mathbb{Y}(t)$

(c) $\mathbb{V}(t)$ **(d)** $\mathbb{Z}(t)$

Figure 2. Persistence dynamics of system (2.12) under the parameter values of Table 1 (Set 2). Panels (a)–(d) display the trajectories of $\mathbb{X}(t)$, $\mathbb{Y}(t)$, $\mathbb{V}(t)$, and $\mathbb{Z}(t)$, respectively, and compare the cases with Lévy jumps, without jumps, and without stochastic noise. The persistence of infected hepatocytes and free virus particles is consistent with the conditional persistence behaviour described in Theorem 6.1.

7.5. Effects of Lévy noise

In this subsection, the influence of Lévy jump noise on the long-term qualitative behaviour of the proposed model is explored through numerical simulations. The analysis is primarily motivated by the role of stochastic perturbations and jump amplitudes in shaping the persistence dynamics of HBV infection. In particular, we investigate how variations in the Brownian noise intensities and Lévy jump amplitudes affect the trajectories of the infected hepatocyte population. To improve the realism of the formulation, model (2.12) incorporates two types of stochastic perturbations, namely Lévy jump noise and Gaussian white noise. To explain their effects, relatively larger values of the noise intensities $\alpha_1, \alpha_2, \alpha_3$, and α_4 are considered, while the remaining parameter values are taken from Table 1 (Set 3). At the same time, relatively large jump amplitudes are chosen as $h_1 = 0.6$, $h_2 = 0.75$, $h_3 = 0.44$, and

$h_4 = 0.33$. Under these conditions, the stochastic model (2.12) exhibits persistent infection dynamics with pronounced random fluctuations. Figure 3 provides a graphical representation of the simulated trajectories supporting this observation. In addition, larger values of the noise intensities generate stochastic paths characterized by jump behaviour and visible fluctuations, as illustrated in Figures 3a–3c.

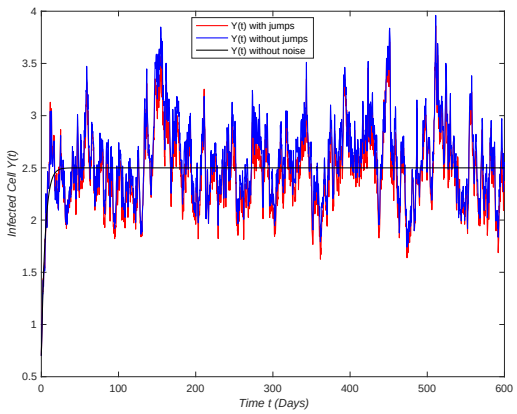

(a) $\alpha_1 = 0.70, \alpha_2 = 0.75, \alpha_3 = 0.50, \alpha_4 = 0.55$

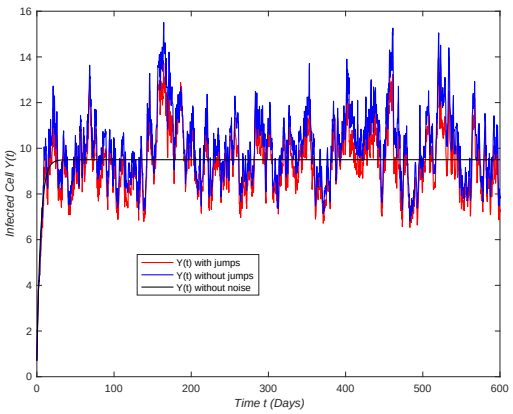

(b) $\alpha_1 = 0.75, \beta_2 = 0.80, \alpha 3 = 0.505, \alpha_4 = 0.40$

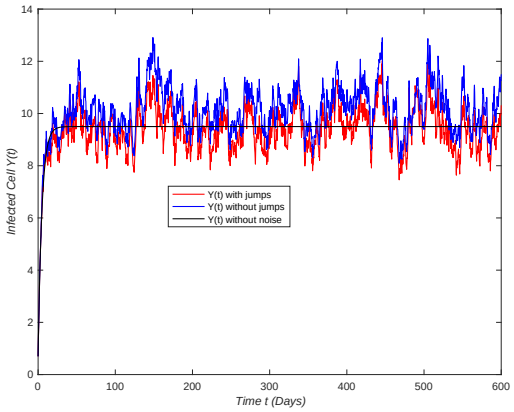

(c) $\alpha_1 = 0.70, \alpha_2 = 0.75, \alpha_3 = 0.30, \alpha_4 = 0.45$

Figure 3. Effects of Lévy jump noise on the infected hepatocyte population $\Upsilon(t)$ under different noise intensities. The simulations use the parameter values of Table 1 (Set 3) and compare the trajectories with jumps, without jumps, and without stochastic noise. Larger noise intensities produce stronger fluctuations and visible jump behavior, illustrating the influence of Lévy perturbations on the persistence dynamics of HBV infection.

8. Conclusions

In this work, we examined a stochastic HBV model with virus-to-cell transmission, cell-to-cell transmission, CTL immune response, Brownian perturbations, and Lévy jump noise. We first established the existence, uniqueness, and positivity of the global solution. The extinction analysis

shows that the infection dies out under the sufficient condition stated in Theorem 5.1. Moreover, a conditional sufficient persistence criterion is obtained under bounded-state dynamics. Numerical simulations support the theoretical findings and show that stochastic perturbations and Lévy jumps can strongly influence the long-term behaviour of HBV infection. Additional numerical reliability tests, including step-size sensitivity, relative error estimation, positivity verification, and comparison with a positivity-preserving truncated Euler-Maruyama scheme, further support the robustness of the simulations.

Although the proposed model provides useful insight into the stochastic dynamics of HBV infection with CTL immune response, cell-to-cell transmission, and Lévy jumps, it has some limitations. First, the model is based on a compartmental structure and therefore simplifies the complex intracellular replication cycle of HBV. Second, the parameters are assumed to be constant, although in real patients they may vary over time due to immune status, treatment response, disease stage, and other biological factors. Third, the stochastic perturbations are introduced through Brownian motion and Lévy jumps to represent environmental and biological fluctuations, but the exact intensity and distribution of such perturbations are difficult to estimate from clinical data. Fourth, the model does not explicitly include antiviral therapy, drug resistance, spatial heterogeneity in liver tissue, or detailed immune components such as helper T cells, B cells, cytokines, and antibody responses. Moreover, the numerical simulations are mainly intended to support the theoretical results and are not fitted to patient-specific data.

Future research may extend the present framework by incorporating treatment effects, time-dependent parameters, distributed or state-dependent delays, fractional-order dynamics, spatial diffusion, and additional immune response mechanisms. Another important direction is to estimate parameters using clinical HBV data and validate the model predictions against patient-specific viral load and immune response measurements. Such extensions would improve the biological realism of the model and may help develop more effective strategies for HBV control and treatment.

Author contributions

F. Mirza, Z. A. Alhussain and J. Feng: Conceptualization; F. Mirza, Z. A. Alhussain and A. Din: Methodology; F. Mirza: Software; F. Mirza, Z. A. Alhussain, J. Feng and A. Din: Validation; F. Mirza and J. Feng: Formal analysis; F. Mirza and A. Din: Investigation; J. Feng and Z. A. Alhussain: Resources; F. Mirza: Writing—original draft preparation; Z. A. Alhussain, J. Feng and A. Din: Writing—review and editing; F. Mirza and Z. A. Alhussain: Visualization; Z. A. Alhussain and J. Feng : Supervision. All authors have read and agreed to the published version of the manuscript.

Use of Generative-AI tools declaration

All authors declare that they have not used Artificial Intelligence (AI) tools in the creation of this article.

Funding

The Researchers would like to thank the Deanship of Graduate Studies and Scientific Research at Qassim University (www.qu.edu.sa) for financial support (QU-APC-2026).

Conflict of interest

All authors declare no conflicts of interest in this paper.

References

1. S. Alchon, *A Pest in the Land: New World Epidemic in a Global Perspective*, UNM Press, 2003.
2. M. Martcheva, Age-structured epidemic models, In: *An introduction to mathematical epidemiology*, Boston, MA: Springer US, 2015.
3. World Health Organization, *WHO COVID-19 Dashboard*. Available from: `https://data.who.int/dashboards/covid19/deaths?n=c`.
4. J. Wang, X. Tian, Global stability of a delay differential equation of hepatitis B virus infection with immune response, *Electron. J. Differ. Equ.*, **2013** (2013), 1–11.
5. M. A. Nowak, R. M. May, *Virus dynamics: Mathematical principles of immunology and virology*, UK: Oxford University Press, 2000.
6. M. A. Nowak, S. Bonhoeffer, A. M. Hill, R. Boehme, H.C. Thomas, H. McDade, Viral dynamics in hepatitis B virus infection, *Proc. Natl. Acad. Sci. USA*, **93** (1996), 4398–4402. https://doi.org/10.1073/pnas.93.9.4398
7. A. S. Perelson, P. W. Nelson, Mathematical analysis of HIV-1 dynamics in vivo, *SIAM Rev.*, **41** (1999), 3–44. https://doi.org/10.1137/S0036144598335107
8. X. Song, A. U. Neumann, Global stability and periodic solution of the viral dynamics, *J. Math. Anal. Appl.*, **329** (2007), 281–297. https://doi.org/10.1016/j.jmaa.2006.06.064
9. L. Min, Y. Su, Y. Kuang, Mathematical analysis of a basic virus infection model with application to HBV infection, *Rocky Mountain J. Math.*, **38** (2008), 1573–1585. https://www.jstor.org/stable/44239519
10. Y. Zheng, L. Min, Y. Ji, Y. Su, Y. Kuang, Global stability of endemic equilibrium point of basic virus infection model with application to HBV infection, *J. Syst. Sci. Complex.*, **23** (2010), 1221–1230. https://doi.org/10.1007/s11424-010-8467-0
11. K. Lv, Y. Zhang, G. Yin, X. Li, M. Zhong, X. Zhu, et al., Extracellular vesicles derived from lung M2 macrophages enhance group 2 innate lymphoid cells function in allergic airway inflammation, *Exp. Mol. Med.*, **57** (2025), 1202–1215. https://doi.org/10.1038/s12276-025-01465-6
12. L. Guo, K. Zhu, Y. N. Zhong, M. Gao, J. Liu, Z. Qi, et al., Structural basis and biased signaling of proton sensation by GPCRs mediated by extracellular histidine rearrangement, *Mol. Cell*, **85** (2025), 1658–1673.e7. https://doi.org/10.1016/j.molcel.2025.03.018
13. Z. Yang, Y. Q. Ping, M. W. Wang, C. Zhang, S. H. Zhou, Y. T. Xi, et al., Identification, structure, and agonist design of an androgen membrane receptor, *Cell*, **188** (2025), 1589–1604.e24. https://doi.org/10.1016/j.cell.2025.01.006
14. Y. Yang, B. Rong, H. Shi, K. Lu, X. Lin, Y. Wen, et al., Rational design of dual PB2/JAK2 inhibitors achieving balanced antiviral and host-directed immunomodulatory effects, *Eur. J. Med. Chem.*, **307** (2026), 118642. https://doi.org/10.1016/j.ejmech.2026.118642

15. J. M. Murray, R. H. Purcell, S. F. Wieland, The half-life of hepatitis B virions, *Hepatology*, **44** (2006), 1117–1121. https://doi.org/10.1002/hep.21364

16. A. Elaiw, N. AlShamrani, Global stability of humoral immunity virus dynamics models with nonlinear infection rate and removal, *Nonlinear Anal. Real*, **26** (2015), 161–190. https://doi.org/10.1016/j.nonrwa.2015.05.007

17. K. A. Aldwoah, M. A. Almalahi, K. Shah, Theoretical and numerical simulations on the hepatitis B virus model through a piecewise fractional order, *Fractal Fract.*, **7** (2023), 844. https://doi.org/10.3390/fractalfract7120844

18. Z. Shi, D. Jiang, Dynamical behaviors of a stochastic HTLV-I infection model with general infection form and Ornstein-Uhlenbeck process, *Chaos Soliton. Fract.*, **165** (2022), 112789. https://doi.org/10.1016/j.chaos.2022.112789

19. S. Ullah, M. A. Khan, M. Farooq, Mathematical modeling of hepatitis B infection with vaccination and optimal control interventions, *J. Comput. Methods Sci. Eng.*, **20** (2020), 331–349. https://doi.org/10.3233/JCM-190028

20. H. Q. Zhang, B. Z. Cao, Q. T. Cao, M. Hun, L. Cao, M. Y. Zhao, An analysis of reported cases of hemophagocytic lymphohistiocytosis (HLH) after COVID-19 vaccination, *Hum. Vaccines Immunother.*, **19** (2023), 2263229. https://doi.org/10.1080/21645515.2023.2263229

21. Y. Jia, B. Fu, L. Dong, M. Zhao, Sweet syndrome induced by SARS-CoV-2 vaccines: A systematic review of patient-report studies, *Hum. Vaccines Immunother.*, **19** (2023), 2217076. https://doi.org/10.1080/21645515.2023.2217076

22. K. Xu, B. Gao, J. Li, Y. Xiang, L. Cao, M. Zhao, Clinical features, diagnosis, and management of COVID-19 vaccine-associated Vogt-Koyanagi-Harada disease, *Hum. Vaccines Immunother.*, **19** (2023), 2220630. https://doi.org/10.1080/21645515.2023.2220630

23. A. Din, Y. Li, A. Yusuf, Delayed hepatitis B epidemic model with stochastic analysis, *Chaos Soliton. Fract.*, **146** (2021), 110839. https://doi.org/10.1016/j.chaos.2021.110839

24. W. A. Khan, R. Zarin, A. Zeb, Y. Khan, A. Khan, Navigating food allergy dynamics via a novel fractional mathematical model for antacid-induced allergies, *J. Math. Tech. Model.*, **1** (2024), 25–51. https://doi.org/10.56868/jmtm.v1i1.3

25. A. Din, Y. Li, Mathematical analysis of a new nonlinear stochastic hepatitis B epidemic model with vaccination effect and a case study, *Eur. Phys. J. Plus*, **137** (2022), 558. https://doi.org/10.1140/epjp/s13360-022-02748-x

26. H. Tahir, A. Din, W. A. Khan, M. ur Rahman, Numerical investigation of a wireless sensor network epidemic model with α-stable noise: A case study, *AIMS Math.*, **10** (2025), 20312–20345. https://doi.org/10.3934/math.2025908

27. S. Ouyang, G. Chen, Y. Xia, G. Shi, Y. Feng, Stochastic dynamics of influenza epidemic model with vaccination strategy, *AIMS Math.*, **10** (2025), 20412–20442. https://doi.org/10.3934/math.2025912

28. S. M. A. Shah, Y. Nie, A. Alkhazzan, C. Tunc, A. Din, A stochastic hepatitis B model with media coverage and Lévy noise, *J. Taibah Univ. Sci.*, **18** (2024), 2414523. https://doi.org/10.1080/16583655.2024.2414523

29. A. Din, Y. Li, Lévy noise impact on a stochastic hepatitis B epidemic model under real statistical data and its fractal-fractional Atangana-Baleanu order model, *Phys. Scr.*, **96** (2021), 124008. https://doi.org/10.1088/1402-4896/ac1c1a

30. J. Li, K. Men, Y. Yang, D. Li, Dynamical analysis on a chronic hepatitis C virus infection model with immune response, *J. Theor. Biol.*, **365** (2015), 337–346. https://doi.org/10.1016/j.jtbi.2014.10.039

31. A. Mojaver, H. Kheiri, Dynamical analysis of a class of hepatitis C virus infection models with application of optimal control, *Int. J. Biomath.*, **9** (2016), 1650038. https://doi.org/10.1142/S1793524516500388

32. W. Mothes, N. M. Sherer, J. Jin, A. Zhong, Virus cell-to-cell transmission, *J. Virol.*, **84** (2010), 8360–8368. https://doi.org/10.1128/JVI.00443-10

33. K. Razali, H. H. Thein, J. Bell, M. Cooper-Stanbury, K. Dolan, G. Dore, et al., Modelling the hepatitis C virus epidemic in Australia, *Drug Alcohol Depen.*, **91** (2007), 228–235. https://doi.org/10.1016/j.drugalcdep.2007.05.026

34. F. Zhang, J. Li, C. Zheng, L. Wang, Dynamics of an HBV/HCV infection model with intracellular delay and cell proliferation, *Commun. Nonlinear Sci. Numer. Simul.*, **42** (2017), 464–476. https://doi.org/10.1016/j.cnsns.2016.06.009

35. M. Sourisseau, N. Sol-Foulon, F. Porrot, F. Blanchet, O. Schwartz, Inefficient human immunodeficiency virus replication in mobile lymphocytes, *J. Virol.*, **81** (2007), 1000–1012. https://doi.org/10.1128/jvi.01629-06

36. B. Monel, E. Beaumont, D. Vendrame, O. Schwartz, D. Brand, F. Mammano, HIV cell-to-cell transmission requires the production of infectious virus particles and does not proceed through Env-mediated fusion pores, *J. Virol.*, **86** (2012), 3924–3933. https://doi.org/10.1128/JVI.06478-11

37. Y. Yang, Q. Han, Z. Hou, C. Zhang, Z. Tian, J. Zhang, Exosomes mediate hepatitis B virus transmission and NK-cell dysfunction, *Cell. Mol. Immunol.*, **14** (2017), 465–475. https://doi.org/10.1038/cmi.2016.24

38. T. Luzyanina, G. Bocharov, Stochastic modeling of the impact of random forcing on persistent hepatitis B virus infection, *Math. Comput. Simulat.*, **96** (2014), 54–65. https://doi.org/10.1016/j.matcom.2011.10.002

39. F. Xie, M. Shan, X. Lian, W. Wang, Periodic solution of a stochastic HBV infection model with logistic hepatocyte growth, *Appl. Math. Comput.*, **293** (2017), 630–641. https://doi.org/10.1016/j.amc.2016.06.028

40. A. Din, Bifurcation analysis of a delayed stochastic HBV epidemic model: Cell-to-cell transmission, *Chaos Soliton. Fract.*, **181** (2024), 114714. https://doi.org/10.1016/j.chaos.2024.114714

41. C. Ji, D. Jiang, Threshold behaviour of a stochastic SIR model, *Appl. Math. Model.*, **38** (2014), 5067–5079. https://doi.org/10.1016/j.apm.2014.03.037

42. M. El Fatini, I. Sekkak, Lévy noise impact on a stochastic delayed epidemic model with Crowley-Martin incidence and crowding effect, *Physica A*, **541** (2020), 123315. https://doi.org/10.1016/j.physa.2019.123315

43. M. Zahri, Multidimensional Milstein scheme for solving a stochastic model for prebiotic evolution, *J. Taibah Univ. Sci.*, **8** (2014), 186–198. https://doi.org/10.1016/j.jtusci.2013.12.002

44. Y. Zhu, L. Wang, Z. Qiu, Dynamics of a stochastic cholera epidemic model with Lévy process, *Physica A*, **595** (2022), 127069. https://doi.org/10.1016/j.physa.2022.127069

45. A. Khan, A. Din, Stochastic analysis for measles transmission with Lévy noise: A case study, *AIMS Math.*, **8** (2023), 18696–18716. https://doi.org/10.3934/math.2023952

46. X. Mao, F. Wei, T. Wiriyakraikul, Positivity preserving truncated Euler-Maruyama method for stochastic Lotka-Volterra competition model, *J. Comput. Appl. Math.*, **394** (2021), 113566. https://doi.org/10.1016/j.cam.2021.113566

AIMS Press